# Back-barrier evolution and along-strike variations in infilling of the Kosi Bay lake system, South Africa

Dladla, N., Green, A. N., Humphries, M. S., Cooper, A., Godfrey, M., & Wright, I. (2022). Back-barrier evolution and along-strike variations in infilling of the Kosi Bay lake system, South Africa. *Estuarine Coastal and Shelf Science*, *272*, [107877]. https://doi.org/10.1016/j.ecss.2022.107877



**Published in:**
Estuarine Coastal and Shelf Science

**Publication Status:**
Published (in print/issue): 05/08/2022

**DOI:**
10.1016/j.ecss.2022.107877

**Document Version**
Author Accepted version

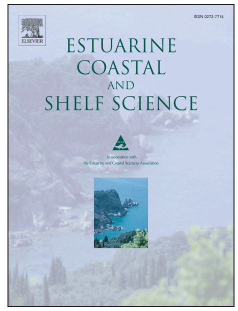


Back-barrier evolution and along-strike variations in infilling of the Kosi Bay lake system, South Africa

N.N. Dladla, A.N. Green, M.S. Humphries, J.A.G. Cooper, M. Godfrey, C.I. Wright

PII: S0272-7714(22)00136-6

DOI: https://doi.org/10.1016/j.ecss.2022.107877

Reference: YECSS 107877

To appear in: *Estuarine, Coastal and Shelf Science*

Received Date: 9 February 2022

Revised Date: 22 April 2022

Accepted Date: 25 April 2022

# Back-barrier evolution and along-strike variations in infilling of the Kosi Bay Lake system, South Africa

N.N. Dladla[a*], A.N. Green[a,b], M.S. Humphries[c], J.A.G. Cooper[a,b], M. Godfrey[a], C.I. Wright[d]

[a]Geological Sciences, School of Agricultural, Earth and Environmental Sciences, University of KwaZulu-Natal, South Africa

[b]School of Geography and Environmental Sciences, Ulster University, United Kingdom

[c]School of Chemistry, University of the Witwatersrand, Johannesburg, South Africa

[d]TERRAMARE LIMITED: Land and Sea GeoSolutions, Christchurch, New Zealand

## Abstract

This study examines both the inlet dynamics, recorded in the back-barrier stratigraphy of Kosi Bay, and the competing effects of waterbody segmentation on along-strike changes in the character and nature of an incised valley fill at Kosi Bay, South Africa. The Kosi Bay system comprises four interconnected lakes (Lake Makhawulani, Lake Mpungwini, Lake Nhlange and Lake Amanzimnyama) subject to varying degrees of marine influence. Formerly, the system's only connection to the ocean was through the Bhanga Nek palaeo-inlet. The location of this system behind a continuous coastal barrier predisposes it to excellent archives of environmental change related to changing sea-level and sediment supply. In this context, two cores were extracted from the system (KB2 and KB4), together with over 150 km of seismic reflection profiling, as well as AMS radiocarbon analyses and legacy data in order to present a new stratigraphic evolution model for this back-barrier system. A total of 5 seismic units were imaged (Units A-E). A major unconformity surface (SB), characterised by broad u-shaped incised valleys, incises the underlying unconsolidated sandy acoustic basement (Unit A). Unit B forms as thickly developed central basin deposits, partially infilling the incised valleys. Two forms of prograding spits are evident−Unit C1 progrades from the palaeo-highs of the valley interfluves into the nearest available accommodation space and Unit C2 progrades from the margins of the system into the basin. These are separated by an erosional surface (T-RS) formed by migrating tidal channels as sea-level rose and marine waters entered the system during the Holocene. Unit C2 spits are in turn associated with slump deposits formed on the steepest part of the margins (Unit D) that were dated to 2900 ± 165 cal. BP. The unusual depth of Surface T-RS is attributed to (1) limited sediment supply during sea-level rise, (2) the presence of easily erodible fine sediments in which this surface erodes and (3) a larger tidal prism when the Bhanga Nek inlet was still open and system segmentation by Units C2 and D had not yet occurred. Unit E caps the stratigraphy and is interpreted as lacustrine fines with a thin layer of acoustically transparent material (gyttja) on top. The deposition of Unit E signifies the closure of the system to the ocean and the overall shift from an estuarine/lagoon environment to a lacustrine one. Recalibrated AMS dates place the system closure to between 3160 and 2900 cal. BP, coeval with the formation of the prograding marginal spits and waterbody segmentation (Unit C2). Along-strike variation in the timing of the basin infilling, attributed to changes to the inlet functioning coupled to the segmentation of the waterbody, is characteristic of this area. At 1450 cal. BP, a new tidal inlet formed to the north of Lake Makhawulani, where impounded waters were diverted via a low point in the back-barrier coastal dune cordon. The formation of this inlet suggests a prolonged period of back-barrier flooding until a low point in the barrier was breached during the Holocene sea-level highstand of 1.5 m. Such inlet development and along-strike back flooding of incised valleys is an unusual attribute of coastal waterbodies of South Africa.

## 1. Introduction

Barrier and barrier-island systems make up about 15% of the World's coastlines (Davies, 1980). Concomitantly, their back-barrier environments comprise significant tracts of the global coastlines and act as key sites of estuaries and wetlands and critical nexus points for groundwater-seawater interaction. Barriers and associated inlets experience various changes in their morphological and sedimentological characteristics over time (Mallinson et al., 2018; Cooper et al., 2018a) because of changing wave and tide energies, sea-level and sediment supply (Hayes, 1979; Riggs et al., 2009; Moran et al., 2015). These changes determine the hydraulic connectivity between back-barrier estuaries/lagoons and the adjacent ocean, thus controlling the tidal range, waves, currents and salinity of the back-barrier estuary/lagoon, as well as the overall morphology (Mallinson et al., 2018). These in turn affect the biological functioning of these systems, many of which are globally recognised as important biodiversity hotspots and zones of species endemism. Critically, morphological changes to a barrier system (such as the number and width of inlets), in addition to the relative timing of inlet closure and development, can also affect areas far removed from the barriers themselves (Mallinson et al., 2018; Green et al., 2022a) Despite this acknowledgement, the fundamental sequence stratigraphic models of incised valleys (e.g. Roy, 1984; Nichols, 1989; Zaitlin et al., 1994) do not recognise the role that multiple inlets to an incised valley may play in creating along-strike variations in the development of a back-barrier sedimentary body. Such considerations are also neglected from models of barrier and back-barrier behaviour that are often two dimensional in nature.

The northeastern coast of South Africa is characterised by several coastal waterbodies that have been linked to the ocean over the last glacial cycle (Wright et al., 2000). Of these, the majority comprise bedrock-incised valleys that have since back-flooded during the postglacial transgression to form lagoons and lakes that are impounded behind a large, immobile and long-lived barrier system (Orme, 1973; Hill, 1975; Wright et al., 2000; Dladla et al., 2019; 2021; Green et al., 2022a). Among these coastal waterbodies are one of Africa's largest estuaries (Lake St Lucia), and South Africa's most pristine estuary (the Kosi Bay system; Ndlovu and Demlie, 2016). Kosi Bay is unique in the sense that its incised valley is hosted in unconsolidated sediment, it is the deepest of all coastal waterbodies in Southern Africa, and is also the one of the least affected by contemporary fluvial drainage inputs and marine sediment supply (Cooper et al., 2012). Its only inlet is ~ 16 km from its most landward inflow point, with most of the freshwater supply to the system derived from groundwater. In describing the Kosi system, Cooper et al. (2012) coined the term "give-up estuary" where such limited sediment supply means that whatever sediment that was supplied was outstripped by the rates of rising sea levels and later back-barrier impoundment of the waters that drowned the incised valley. Consequently, the infilling processes are mostly limited to organic detritus and very little marine materials.

In this light, the back-barrier stratigraphy is particularly sensitive to phases of marine connection, as most sandy materials are sourced via the palaeo-inlets that connected the lakes to the ocean. Coupled to this are other back-barrier changes related to periods of stability such as segmentation (Cooper et al., 2012), which formed spits and barriers that may amplify or diminish the along-strike tidal prism and, accordingly, its record in the back-barrier depositional sequence. Changes related to inlets, lagoon segmentation and sedimentation may all thus influence the ecology of the back-barrier over time.

In this paper we use newly acquired seismic stratigraphic data, long piston cores, AMS radiocarbon analyses, and legacy data to present a new stratigraphic model for the back-barrier evolution of the system. We examine both the inlet dynamics, which is well recorded in the back-barrier stratigraphy of Kosi Bay, and the competing effects of waterbody segmentation on along-strike changes in the character and nature of the incised valley fill.

## 2. Regional setting

### 2.1. Physiography

The Kosi Bay lake system (approximately 26º 53'S to 27º 02'S and 32º 48' E to 32º 53'E) is situated in northern KwaZulu-Natal (KZN) on the east coast of South Africa (Fig. 1a and c; Wright et al., 2000). It comprises four interconnected lakes (Lake Makhawulani, Lake Mpungwini, Lake Nhlange and Lake Amanzimnyama), separated from each other by sandy barriers (Fig. 1a). Lake Nhlange is the largest of the four lakes, occupying an area of 31.4 $km^2$ (Wright et al., 1997). It reaches a maximum depth of ~ 27 m with most of the deeper areas covered in gyttja and enclosed by sandy spits (Wright et al., 2000). The smaller lakes are shallower, and similarly act as focal points for gyttja accumulation. The lake systems are supplied by several ill-defined rivers, with just the Sihadhla River, which drains into Lake Amanzimnyama, and the Gesiza River, which drains into lake Nhlange, being perennial. The lakes are mostly supplied by groundwater seepage (Ndlovu and Demlie, 2016) with very little suspended sediment entering the system.

To the west, the Kosi system is bound by mid- to late Pleistocene red to orange semi-consolidated dune sands, forming cliffs (Wright et al., 1999), and to the east, a large coastal dune complex separates the Kosi Bay system from the Indian Ocean (Wright et al., 1999). This dune barrier comprises a core of red dune sands which are Pleistocene in age (Du Preez and Wolmarans, 1986; Botha and Porat, 2007). Against these, yellowish and white Holocene age dune sands then accumulated (Cooper et al., 1989).

Beneath the Pleistocene to Holocene sediment cover lie Tertiary and Cretaceous age argillaceous sediments (Wright, 1995; Botha, 2018). Presently, the system's connection to the sea occurs via a single tidal inlet north of Lake Makhawulani (Cooper et al., 2012; Fig.1a). This present-day inlet formed during a sea-level highstand at +1.5 m, ~ 1600 BP (Wright et al., 2000). This was established on the basis of a beachrock landward of the modern inlet, the date of which is recalibrated here to 1450 ± 140 cal. BP) (Fig. 1b; Table 1). This followed the permanent closure of an inlet to the south that previously connected Lake Nhlange to the ocean at Bhanga Nek (Cooper et al., 2012) ~ 3000 BP (uncalibrated).

## 2.2. Climate and hydrodynamic regime

Subtropical and temperate inland climates dominate the coastal plain (Wright et al., 2000). The mean annual temperature in Kosi Bay is 21.6 ºC, reaching a minimum of 11.6 ºC in winter and a maximum of 28.7 ºC in summer (Cooper et al., 2012). Coast-parallel winds are dominant; in summer, north to north-easterly winds prevail, whereas both north-easterly and south-westerly winds occur during the winter period (Diab and Sokolic, 1996; Wright, 1999). The coastline is strongly wave-dominated and sediment starved. It is dominated by the swift, southward flowing Agulhas Current (Flemming, 1978; Lutjeharms, 2006) that sweeps the shelf to depths of 20 m offshore the study area (Green et al., 2022b). Large-amplitude south-easterly swells characterise the wave climate (Rossouw, 1984). However, when north-easterly winds occur, lower amplitude swells prevail (Van Heerden and Swart, 1986). The tides are semi-diurnal, with an average tidal range of approximately 1.8 m (SAN, 2009).

## 3. Methodology

A geophysical and sedimentological survey of Kosi Bay was undertaken in which high-resolution, single channel seismic data were acquired throughout the back-barrier system. The collection of these seismic data was accompanied by the extraction of two piston-cores from Lakes Mpungwini and Amanzimnyama.

### 3.1. Seismic reflection data

This study focuses on seismic reflection data collected from Lake Mpungwini and Lake Nhlange (Figs. 2-8). The seismic reflection profiles were collected using a broad frequency boomer sound source (median frequency 600 Hz) at a power level of 175 J. The data were recorded using a Coda D4AG digital acquisition system, coupled to a real time kinematic differential GPS, with a positional accuracy of ~ 10 cm in the X, Y and Z domains. The raw seismic data were processed using the Hypack™ SBP utility. Bandpass filtering (300-1200 Hz) and time-varied gains were applied to all the data. The data were corrected for streamer offset between the source and GPS and constant sound velocities of 1500 $ms^{-1}$ (in water) and 1650 $ms^{-1}$ (in sediment) were used to extrapolate the time-depth conversions. All data were interpreted according to standard seismic stratigraphic principles (Mitchum and Vail, 1977).

The seismic survey was hindered by: (1) the shallow margins of the lake (< 0.5 m water depth); (2) several shallow sand-banks, which caused pronounced multiple masking of the upper packages of sediment (Fig. 2-8); (3) the presence of a gas-rich calcareous mud (gyttja) in deeper waters that obscures the seismic signal due to strong density contrast (Weschenfelder et al., 2016). As a result, the seismic stratigraphy from the shallower lakes Amaninzyama and Makhawulani could not be examined.

### 3.2. Core data

Two cores, KB2 and KB4 (Fig. 10), were collected using a barge-mounted Uwitec piston corer with a 72 mm diameter barrel, coupled to a percussion drill. Core KB2 (26.942835 S; 32.857184 E) is 8 m long and was collected from Lake Mpungwini (Fig. 1a), from a water depth of 16 m. Core KB4 (27.029221 S; 32.823091 E) is just under 10 m long and was collected from Lake Amanzimnyama (Fig. 1a) from a water depth of approximately 2 m. The cores were split in the laboratory and described according to standard sedimentological procedures. KB2 and KB4 were sub-sampled for inorganic grain size analyses at 4 cm and 5 cm intervals, respectively. A total of 316 sub-samples (133 from KB2 and 183 from KB4) were treated and analysed. All carbonate and organic material was removed prior to analysis using 10% hydrochloric acid and 30% hydrogen peroxide, respectively. The samples were then rinsed and allowed to settle after which they were analysed using a Malvern Mastersizer 2000 to accurately measure the grain-size distributions, on the basis of which mean grain size, sorting and skewness coefficients were determined.

Three samples were taken from each core for AMS radiocarbon dating to build a chronostratigraphic framework. Dating was carried out on bulk organic carbon samples and, where possible, well-preserved whole shells. Analyses were carried out by Beta Analytic Incorporated, Florida, USA. In addition, the cores and $C^{14}$ dates described by Wright et al. (1999) were integrated into this study. This included three cores from Lake Nhlange which intersected the seismic lines described below. All $C^{14}$ dates, including the previously uncalibrated dates of Wright et al. (1999), were calibrated using the Southern Hemisphere atmospheric curve SHCal13 (Hogg et al., 2013) (Table 1). Some of Wright et al.'s (1999) cores are not presented here as they do not intersect our seismic, however recalibrated dates from these are presented in Table 1 in order to standardise the chronology.

## 4. Results

### 4.1. Seismic stratigraphy

Table 2 highlights the 5 seismic units (Unit A-E) that were revealed beneath Lake Mpungwini and Lake Nhlange (Figs. 2-8). Each unit was identified based on the bounding reflectors, the internal reflector arrangements, reflection impedances or amplitudes and the reflection termination patterns.

Key stratigraphic surfaces and sediment thicknesses

Two key erosional surfaces are recognised from the seismic stratigraphy, SB and T-RS. Surface SB is characterised by incisions up to approximately 1100 m-wide and 35 m-deep (Fig. 9a) and forms a particularly deep, coast-parallel channel on the landward side of the barrier. It extends between Lake Nhlange and Lake Mpungwini where it reaches a maximum depth of -17 m. Smaller and less well-defined channels incise to ~ -26 m and produce a disordered drainage pattern, with a coast-perpendicular channel oriented toward Bhanga Nek and a smaller offshoot of this oriented toward Lake Amanzimnyama (Fig. 9a). Surface T-RS is similarly characterised by incisions, however, these are mostly not as deep nor as wide as those of SB (Fig. 9b). A notable exception is a coast-parallel channel along the northeastern margin of Lake Nhlange that is almost of comparable depth to that of SB, reaching -32 m, with a maximum width of approximately 260 m and extending southward toward Lake Amanzimnyama (Fig. 9b). The coast-perpendicular channel is more obvious in T-RS, extending clearly to Bhanga Nek (Fig. 9b). The channels are confined by shallow interfluves that to some extent mirror the modern-day bathymetry (Fig. 9c). The contemporary bathymetric surface reflects the same coast-parallel and coast-perpendicular arrangement of low points in elevation, with some modification.

The post-SB sediment accumulation is marked by thick depocenters attached to the margins that form basin-narrowing wedges into Lake Nhlange (Fig. 9d). These reach up to 28 m in thickness in the northeastern margin of Lake Nhlange and are mostly 10-20 m thick along the southwestern, southeastern and northwestern margins. Several of these thick accumulations occur within the depressions in the SB surface. The post-SB sediment thickness in the central portions of the basin is significantly lower, with sporadic, up to 5 m thick deposits. The sediment accumulation between SB and T-RS appears to be mostly the same as that post-SB to present day (Fig. 9e). A notable exception is that the thick deposit to the northeast, evident in the post-SB isopach, is absent, implying its development after the T-RS formed.

Unit A

Unit A forms the acoustic basement to the study area and is characterised by discontinuous and chaotic, moderate amplitude reflectors with no particular reflection configuration (Fig. 4). These reflections are erosionally truncated by Surface SB and dip in random, often opposing directions. The maximum thickness of this unit cannot be determined but is at least 50 m.

Unit B

Unit B fills the incisions in Surface SB. Unit B is thickly developed and occurs throughout the study area, characterised by concave upwards, aggrading reflectors of moderate to low amplitude that form an onlapping drape with the valley margins (Figs. 2-8a). Where Unit B forms in association with deep valleys, the lower portions of the unit may be obscured by gas blanking (Fig. 7).

Unit C and D

Steeply dipping and prograding, moderate to high amplitude, oblique-parallel reflectors comprise Unit C. This unit may be further subdivided into two sub-units (C1 and C2) which occur sporadically throughout the study area (Figs. 2b-4 and 6-8). Unit C2 overlies Unit C1 and they are separated by Surface T-RS (Fig. 3). Unit C1 mantles Surface SB (e.g. Fig. 3) and may occasionally crop out at the seabed in the absence of T-RS (Fig. 2b), or is erosionally truncated by T-RS. Unit C1 is ≤ 6.5 m thick and progrades into the basin from the channels and valley interfluves of Surface SB (Figs. 3 and 6). In contrast, Unit C2 is mostly ≥ 10 m thick and progrades into the basin from the margins of the system (Figs. 2-4 and 8).

Intercalated within, beneath or below Unit C, is Unit D. Unit D comprises steeply dipping, chaotic, high amplitude, oblique-parallel to sigmoidal reflectors that can merge upslope with Unit C, though the precise contact between the two is unclear and they likely interfinger (Figs. 2a, 4, and 8). Unit D downlaps Surface SB (e.g. Fig. 4) or Surface T-RS (e.g. Fig. 8b) and is overlain by Unit E (Figs. 2a, 4, and 8). The internal reflections of Unit D are characterised by internal discontinuities with small ≤ 2 m offsets and localised deformation at the unit-toe (e.g. Fig. 4).

Unit E

Unit E is laterally extensive and caps the entire stratigraphy (Figs. 2-8). This unit is characterised by parallel, aggrading, low to moderate amplitude reflectors that drape all other units and form the modern-day lake floor. Unit E varies in thickness, ranging from ~ 1.8- 9 m. This unit is often associated with strong gas blanking (e.g. Fig. 2a). In the deeper portions of both Lake Mpungwini and Nhlange, Unit E may be overlain by a thin (~ 1-2 m) layer of acoustically transparent material (e.g. Fig. 2).

## 4.2. Lake Mpungwini and Amanzimnyama cores

Core KB2

The position of Core KB2 in the context of the seismic sections is shown in Fig. 2a. The lower 2 m of the core correlates with Unit B and the remainder correlates with Unit E (Fig. 10a1). The very topmost 2 m comprise the acoustically transparent material at the top of Unit E. KB2 mostly comprises muddy materials characterised by an abundance of shell fragments (Fig. 10a1) and inorganic sediments with a mean grain size less than 63 μm that are poorly sorted (phi values between 1.2 and 2) with symmetrically to positively skewed grain-size distributions (Fig. 10a2-4).

The basal unit (~ 8 - 7.25 m) is composed of very stiff organic-rich clay, which is weakly laminated at the top. Directly overlying this unit (7.25 - 5.5 m) is a sloppy mud, the base of which comprises scattered shells of *Dosinia hepatica*. This unit gradually grades to a silty clay unit with abundant shell debris, with a fine-grained sand lens present at ~ 6 m, marking T-RS. This unit is associated with a slight increase in mean grain size, decrease in sorting and generally near symmetrical grain-size distributions (between - 0.1 and 0.1 phi) with occasional negative and positive spikes. There is an ~1 m thick gap in the core from ~5.5 to 4.5 m. Stiff muds are present from 4.5 to 3.6 m. This unit is overlain by a 1.6-m-thick unit of alternating organic-rich stiff clay and well-laminated silty layers with occasional shells, punctuated by layers of quartz-rich sand and lithic fragments (beach rock) at ~2.6 m and 2.2 m respectively. On average the sediment in this unit has a mean grain size of less than 30 μm with occasional coarser peaks and symmetrical grain-size distributions. The top section of the core is 2 m thick and comprises rhythmically interbedded dark brown and lighter brown-grey varved organic-rich muds, with numerous broken shell fragments. Here, the sediments show a further decrease in mean grain size, an increase in sorting and more positively skewed spikes.

Overall, the core fines upward and becomes better sorted and more positively skewed towards the surface. Repeated spikes from 15 to 30 μm in the mean grain size are evident with greatest variability in the lower 2.5 m of the core. The AMS $C^{14}$ analyses at 0.4 m, 3.52 m and 7.34 m dated to 490 ± 30 cal. BP, 1250 ± 30 cal. BP and 2890 ± 30 cal. BP respectively.

Core KB4

Core KB4 comprises a stiff, organic-rich clayey sediment abundant in bioclastic debris which mostly occurs as finely disseminated, indeterminable shell fragments (Fig. 10b1). The basal unit is ~0.7 m thick and is composed of medium sand (Fig. 10b2). This sandy unit is characterised by sorting that fluctuates between very poorly sorted to moderately well sorted (Fig. 10b3). The following 3 m of the core comprise poorly sorted clayey-silt and clay-rich sediment characterised by symmetrical grain-size distributions (Fig. 10b4). This core section is, however, punctuated by lenses of sand and shell fragments. From 6 to 4 m, the core comprises a clayey-silt with an upward decreasing shell fragment abundance, and occasional, 5 cm-thick sand horizons. This unit is poorly to very poorly sorted and is negatively skewed. The last 4 m of the core comprise a light-grey silty clay with a mean grain size of 63 µm or less (Fig. 10b1 and b2). This sediment is poorly sorted and positively skewed (Fig. 10b3 and b4).

Like KB2, the core fines upward with a notable and regular variation from 10 µm to 40 µm in mean grain size in the upper 9 m. There are abundant shell fragments throughout the core, with occasional whole valves of *Loripes clausus* in the basal sand unit. AMS $C^{14}$ dates from 1.5 m, 5.5 m and 9.02 m correspond to 760 ± 45 cal. BP, 2981 ± 100 cal. BP and 4368 ± 83 cal. BP respectively (Table 1).

4.3. Lake Nhlange cores

Wright et al. (1999) provide a detailed description of five short (> 2.5 m) cores (Core 1-5) collected from Lake Nhlange. Here, we provide a brief re-description of three of these cores and their context in the seismic stratigraphy (Fig. 11; Core 1, 3 and 5), as well as a newly calibrated radiocarbon date from one of the cores (Core 3).

Core 1 (Fig. 11a) was located at a depth of 20 m below mean sea-level and intersects Unit D (Fig. 8a). This core comprises a lowermost unit (2.5 - 2 m) of muddy sand with molluscs (*Solen cylindraceus, Dosinia hepatica, Eumarcia paupercula*). This is overlain by a thin layer of pelleted clayey mud with sand filled burrows. Overlying this is a 0.45 m thick layer of slightly muddy sand. A thin layer of grey black muds separates this unit from the overlying unit. The overlying 0.7 m thick unit comprises white sand with occasional shell fragments. This is in turn overlain by an ~ 0.30 m thick silty mud. The upper two units comprise medium to fine sand which lacks shell fragments.

Core 3 (Fig. 11b) was located at a depth of 28 m below mean sea-level and similarly intersects Unit D (base; 2.3 - 1.4 m) and Unit E (upper portion of the core; 1.4 - 0 m) (Fig. 4). This core comprises a mixture of very fine to medium sand and mud, with forams and shell fragments. A shell-rich layer (*Rhinoclavis kochi, Paphia textile, Fulvia fragilis, Polinices didyma, Bulla ampulla, Dosinia hepatica and Loripes clausus*) at the base of this core was dated at 2900 ± 165 cal. BP. The palaeontological assemblages of the core were considered representative of subtidal lagoonal/estuarine conditions overall (Wright et al., 1999). The boundary between Unit D and E is marked by a sharp/erosional contact lined with rounded mudballs.

Core 5 was located at a depth of 13.5 m below sea-level and is 1.32 m long, penetrating Unit E (Fig. 4). The core comprises a basal muddy, very fine sand unit with shell fragments, overlain by a fine sand with thin black organic mud layers (Fig. 11c).

## 5. Discussion

### 5.1. Seismic stratigraphic interpretation

#### 5.1.1. Kosi Bay Formation sediments and the LGM lowstand

Unit A can be traced from the seismic data directly to cliffs where it crops out as semi-consolidated sediments of the palaeo-coastal dune Kosi Bay Formation. Reworked remnants of these sediments form the present day barrier dune complex to seaward (Botha, 2018). Surface SB occurs throughout the study area, cutting into these underlying semi-consolidated sediments to form an incised valley network, over which later transgressive sequences have been deposited. This surface is pervasive throughout the south-east African coastline (Green, 2009, 2011; Green et al., 2013; Benallack et al., 2016; De Lecea et al., 2017; Dladla et al., 2019, 2021) and is associated with the Last Glacial Maximum (LGM) lowstand when sea levels fell ~130 m below present ~23000-18000 BP (Ramsay and Cooper, 2002; Cooper et al., 2018b). Along most of the region, these LGM-age incised valleys cut into competent bedrock and are mainly characterised by steep, v-shaped valley walls. However, in Kosi Bay, these form as u-shaped and broader incised valleys with little distinct form (e.g. Fig. 6). The incised valley shape and geometry here is like the incised valleys from the Cape Hatteras region of North Carolina, or the northern Gulf of Mexico, where rivers have similarly incised into sandy coastal plain sediments

(Fig. 12; Zaremba et al., 2016; Mattheus and Rodriguez, 2011) and where the lack of bedrock control produces such broad and shallow features.

5.1.2. Central basin deposits

Unit B, which forms the incised valley fills, onlaps and drapes the incised valley walls. This thickly-developed unit (up to 18 m thick) is characteristic of the incised valley systems in coastal waterbodies along the north-east coast of South Africa (Benallack et al., 2016; Dladla et al., 2019, 2021) identified as the central basin deposits of a wave-dominated estuary (Zaitlin et al., 1994) or mixed wave- and tide-dominated estuary (Allen and Posamentier, 1994). Where Unit B is penetrated by KB2, the core comprises organic-rich fines that date to at least 2890 ± 30 cal. BP indicating a persistent marine influence into the central basin to that point.

5.1.3. Prograding Spits

Unit C is characterised by prograding, oblique-parallel reflectors which downlap Surface SB. These prograding packages mimic the appearance of spits developed along the east coast of South Africa (e.g. Wright et al., 2000; Dladla et al., 2019, 2021) as well as globally (e.g. Simms et al., 2010; Nutz et al., 2015; Bortolin et al., 2018). These spits are formed by wind-driven sediment reworking of the shorelines that feed the process of waterbody segmentation (Zenkovich, 1959). Unit C1 progrades from the palaeo-highs of the valley interfluves into the nearest available accommodation space, like those documented in Patos Lagoon, Brazil (Bortolin et al., 2018). This indicates formation during lower than present lake levels, when the back-barrier lagoon margins were being modified by wind-generated waves in the early stages of segmentation, a process that was previously regarded (Wright et al.,1997, Cooper et al., 2012) as having occurred mainly after Holocene sea levels reached the present.

Like Unit C1, Unit C2 also occurs as a series of prograding spits. However, unlike those of Unit C1, these spits prograde from the margins into the basin and are associated with now higher lake levels when the incised valley and proto-lagoon of the Kosi Bay system was drowned by transgressing sea levels. This prograding unit clearly postdates Surface T-RS, as seen in the northeastern portions of the estuary. A similar deep-water prograding sediment body is described in the Baltic Sea by Rucińska-Zjadacz and Wróblewski (2018) and is suggested to be influenced by gravity-driven processes as the spit prograded. Rucińska- Zjadacz and Wróblewski (2018) state that although a few studies on spits prograding into deep water do exist (e.g. Davidson-Arnott and Conliffe, 1994), these are not associated with gravity-driven mass movements. Such a stratigraphic arrangement in the study area seems to be related to the depth of the receiving basin and the high rates of local sediment supply causing the system to produce thick and steep wedges prone to instability.

5.1.4. Margin slump deposits

Unit D forms steeply dipping, prograding wedges. These are chaotic and characterised by localised deformation at the wedge-toe. The seismic nature of this unit resembles slump deposits that have formed on the steepest part of the margins and is closely associated with the prograding Unit C2 spits.

This slumping of the system is a characteristic feature in the Kosi Bay system and is thought to have formed by margin instability associated with wave reworking of lagoonal and lacustrine shorelines (Wright et al., 1999; Cooper et al., 2012). These slump packages have some similarities to those typically formed on delta fronts of bayhead deltas, however, they are different from delta front processes (Rucińska-Zjadacz, and Wróblewski, 2018) where sediment delivery to the steep margins usually occurs through fluvial discharge (e.g. Dladla et al., 2021). In Kosi Bay, undercutting and destabilisation of the unconsolidated aeolian dune sand margins produced a relatively unique fill for an incised valley system. The unstable and deformed prograding barrier spit from the Baltic Sea, described by Rucińska-Zjadacz and Wróblewski. (2018), can broadly be compared to the prograding marginal spits (Unit C2), marked by slumping (Unit D), in the Kosi system.

Core 3 penetrated this slumped material, and notably comprises estuarine molluscan assemblages such as *Dosinia hepatica* and *Loripes Clausus*. We consider that the core material was initially deposited in a shallow subtidal sandy environment that formed the spit platform, before being transported into the parts of the system > 30 m depth. The base of this material was dated to 2900 ± 165 cal. BP constraining the age of the slumping to after this time period. This timing overlaps a period of significantly drier climate in SE Africa between 3700 and 2600 cal. BP (Humphries et al., 2019). We suggest that at this time, the presumably lowered lake levels would have exposed the sandy shorelines to significant reworking and spit development producing a more segmented waterbody. A similar example is documented in the Lake St Lucia system 140 km to the south, where drought phases resulted in increased wind-driven spit development and lagoon segmentation (Humphries et al., 2016; Green et al., 2022a). This increased sediment supply to the spits, coupled with their progradation into deep water (≤ 25 m), resulted in the oversteepening of the margins of Unit C2. This led to slumping of the spits, producing Unit D along the steep margins. Further, prior to segmentation, the wind fetch of the system would have been far greater (along coastal strike), conditioning the system for segmentation once the lake levels were optimal.

5.1.5. Lacustrine fines

Unit E caps the stratigraphy and is characterised by aggrading, low amplitude draped reflections, indicative of a low-energy depositional environment. Similar deposits have been found in Lake St. Lucia and were recognised as the lacustrine backfill of the system (Benallack et al., 2016; Dladla et al., 2019). The upper positions of Unit E also comprise acoustically transparent materials, or materials with high acoustic opacity due to gas. These correspond to gyttja deposits in Lake Mpungwini, e.g. the upper 1.5 m of KB4 was deposited since at least >1250 ± 30 cal. BP (Fig. 10a1). The deposition of Unit E signifies the closure of the system to the ocean, and the shift from an estuarine/lagoon environment to a lacustrine environment, starved from clastic sediment sources from both fluvial and marine inputs. This has been observed, for example, in the Patos Lagoon of Brazil, where tidal inlets closed during the

Holocene highstand, and the resultant deposition was characterised by draping of fine sediments (cf. Bortolin et al., 2018).

5.2. Core data interpretation and the timing of open inlets

Previous dating of the uppermost estuarine sediments in Lake Nhlange, yielded ages between 3160 ± 200 and 2900 ± 165 cal. BP (recalibrated from Wright et al., 1999). Cooper et al. (2012) suggested that these marked the closure of the Bhanga Nek inlet and a shift to lacustrine conditions, and that this closure was permanent and associated with falling sea levels after a late Holocene high at approximately 4500-5000 BP. The timing in deposition, however, places these in a period when sea level was relatively stable ~ +1 m above present (Fig. 1b) (Cooper et al., 2018b).

Core KB4 reveals two main units, a basal tidal sequence characterised by medium sands containing the estuarine bivalve *Loripes clausus*, followed by an erosional boundary (Surface T-RS?) and then the overlying fines which we interpret as the lacustrine unit, interposed with occasional sandy lenses, and capped by gyttja-rich muds.  The sandy basal unit would have been deposited during an open inlet phase, with the overlying AMS date from these lacustrine fines indicating the onset of lacustrine deposition at ~ 4400 cal. BP. We consider the basal sandy marine materials in core KB4 of Lake Amanzimnyama to be sourced from the Bhanga Nek inlet. The core location (Fig. 1a) is ~ 5 km from the old inlet at Bhanga Nek, a distance equivalent to the limit of the contemporary flood-tide sediments in Lake Makhulawani from the modern inlet (Cooper et al., 2012).

The difference in the timing of the onset in lacustrine conditions in Lakes Amanzinyama and Nhlange can be ascribed to segmentation that occurred whilst the Bhanga Nek inlet was open. The enclosure of Lake Amanzinyama by spit growth of Unit C2 buffered, and diminished, the tidal prism into the lake, thus promoting relatively lower energy conditions to begin earlier. This also accounts for the nearly 9 m of sediment that since accumulated, as compared to the thin, post inlet-closure accumulations in Lake Nhlange.

The overall coarser, more poorly sorted and more negatively skewed sediment at the base of KB2 dates to 2890 ± 30 cal. BP, which is within error for the dates on the Bhanga Nek closure and predates the development of T-RS. The post-TRS sediment is finer, less poorly sorted and more positively skewed upcore. As with core KB4, the regular cycle of peakiness in grain sizes, coupled to small reductions in the skewness co-efficient suggests the addition of coarser materials without winnowing of the receiving basin sediment. A similar phenomenon was presented by Humphries et al. (2019 and 2020) for the Muzi Pan and Mkuze River deltas and was ascribed to increased periods of aridity and deflation of material form the seaward barrier. Pending a more detailed radiocarbon analysis, this same resolution in the reconstruction of the palaeo-hydroclimate cannot yet be achieved.

### 5.3. An unusual tidal ravinement surface?

Surface T-RS is found throughout the study area, with several incisions of various depths. This surface formed after the deposition of the main incised valley fill and in some cases has exhumed these sediments almost to the depth of the subaerial unconformity (SB) (Fig. 9 b). Apart from the LGM surface (SB), Wright et al. (2000) also recognised another prominent and laterally extensive reflector which they interpreted as a transgressive-regressive erosional surface in Lake Nhlange. They suggested that this surface represented the regression from the mid-Holocene highstand (~ 4500 BP-uncalibrated) when sea levels were 3.5 m above present level (Cooper et al., 2018b). Considering the numerous incisions and variability in incision depth, we instead interpret this surface as a tidal ravinement surface formed as tidal channels migrated during the prolonged back flooding of the incised valley (e.g., Catuneanu et al., 2009; Green et al., 2015; Benallack et al., 2016; Dladla et al., 2019, 2021). Furthermore, the sharp/erosional contact between Unit D and E, lined by rolled mudballs, lends further credence to this interpretation (Fig. 11b), considering that ravinement surfaces are typically lined by lag materials (Zecchin and Catuneanu, 2013). Our newly calibrated dates indicate this period to span up from 2980 cal. BP to 3160 cal. BP.

The depth to which the tidal ravinement incises is related to the tidal range as well as the current energy within the tidal channels (Scasso and Cuitiño, 2016). Miner et al. (2007) suggest that tidal ravinement depths increase with time in response to an increase in the tidal prism, which appears counterintuitive to the Kosi system, where we expect a diminished tidal prism with segmentation. Tidal ravinement surfaces may erode very deeply in some macrotidal or hypertidal settings (e.g. Allen and Posamentier, 1994), though again at odds with the overall upper microtidal setting of the area. In certain cases, tidal channels may also completely exhume the underlying incised valley fill, cutting down to the subaerial unconformity surface in sediment starved estuaries (e.g. Chaumillon et al., 2010; Tessier, 2012). Prolonged periods of low sedimentation rates may further result in extensive migration of tidal channels as these seek to attain a base-level equilibrium (Scasso and Cuitiño, 2016).

Considering how similar the modern bathymetry is to that of the T-RS surface, and in accordance with Cooper et al.'s (2012) identification of the very limited fluvial and marine inputs to the Kosi system, we attribute the unusual depth of the T-RS in Kosi Bay to a combination of the following: (1) limited sediment supplied to the area during transgressing sea levels, (2) the presence of easily eroded fine sediments in which these incisions are hosted as well as (3) a larger tidal prism attributed to the Bhanga Nek inlet and when the system segmentation by seismic Units C2 and D had not yet occurred, thus fostering larger back-barrier water volumes.

The along-strike variation in timing of the basin infilling is here ascribed to changes to the inlet functioning coupled to the segmentation of the waterbody. The segmentation process is dictated by wind-driven circulation along the sandy margins of the system, coupled to the diminishing inlet influences and falling sea levels that expose successively lower shorelines. These operate in feedback loops; once segmentation starts in the system, areas begin to further experience diminished tidal exposure and as such the sedimentary response. In areas most proximal from the inlet, or most sheltered by segmenting bodies, this manifests as areas of increased sedimentation rates, and a reduced grain size.

Infilling is thus in many ways controlled by along-strike changes to the tidal effects, here strongly driven by segmentation, especially so in the absence of multiple marine sources, and strongly diminished fluvial input.

5.4. Evolutionary model

In this section, we summarise the stratigraphic evolution of the Kosi Bay system (Fig. 13), providing a series of temporal reconstructions of the geomorphology and sedimentology from the LGM to present.

Initially, the Kosi Bay system was connected to the ocean via an incised valley that crossed the Bhanga Nek area (Fig. 13a). A single episode of incision occurred during the LGM, cutting into the unconsolidated sediments of the Kosi Bay Formation, extending seaward through Lake Nhlange and diverting along-strike behind the barrier at Lake Mpungwini (Fig. 13a). Whether this along-strike extension is a palaeo-depression in the dunes of the Kosi Bay Formation, or a channel that extends seaward at some point to the north, is not clear due to the limited seismic records in the other lakes and to seaward, however it does bear some morphological resemblance to interdune depressions from the modern dunes of the region (Jackson et al., 2014).

Post-LGM transgressive infilling of the incised valleys deposited 10-18 m thick, homogenous central basin fills (Unit B; Fig. 13b). Due to limited sediment supply during transgression, these only partially filled the incised valleys. With active wind-driven currents, several spits developed (Unit C1), at lower sea levels, which signified the early stages of lagoonal segmentation (Fig. 13b).

A large tidal prism, due in part to a more open back-barrier setting as is currently the case, coupled with the limited sediment supplied resulted in the formation of an unusually deeply-incised tidal ravinement surface (T-RS) (Fig. 13 c), truncating the underlying spits. A sea-level fall from the Holocene maximum at 5000 BP, resulted in further segmentation of the system, coupled to a reduction in the tidal prism. These combined effects initiated the onset of lacustrine conditions in Lake Amanzinyama at 4400 cal. BP, and the eventual closure of the Bhanga Nek inlet between 3160 and 2900 cal. BP (Fig. 13c).

This period was coeval with the development of another series of thick and unstable spits (Unit C2) along the margins of the system, separated from the Unit C1 spits by the tidal ravinement (Fig. 13d). These formed the main sediment depocenters at the time and further reduced the effects of tides into the system sub-depocenters. During the post Holocene-high period of relative sea-level stability, an increase in arid conditions at ~2900 cal. BP led to an increase in sediment supplied to the marginal spits, with eventual deformation and slumping (Unit D) (Fig. 13d). This was coeval with the overall decrease in the energy of the depositional environment, which led to the deposition of draping lacustrine fines and above which a thin layer of gyttja deposits cap the stratigraphy. At 1450 cal. BP, a new tidal inlet formed north of Lake Makhawulani, the formation of which is consistent with the last Holocene sea-level highstand of 1.5 m at ~ 1500 BP (Wright et al., 1997). This suggests a prolonged period of back-barrier flooding until a low point in the barrier was breached during this smaller peak in sea-level (Cooper et al., 2012). Like the situation in Lake St. Lucia (Green et al., 2022a), this present-day inlet bears no relationship to former incised valleys in the system and is rather the result of back-barrier water impoundments.



## 6. Conclusion

The Kosi Bay's back-barrier system has evolved in the context of limited sediment supply, lagoonal segmentation and changes related to tidal inlets over time. Palaeo-coastal dune sediments were incised during the LGM, forming broad u-shaped valleys in the unconsolidated sediment which were partially filled during subsequent transgressing sea levels. Limited sediment supply to the basin resulted in a mixture of spit progradation and gyttja development as the main transgressive sequences apart from some central basin fills in the basal portions of the valley. An unusually deeply-incised tidal ravinement surface characterises the area, formed due to a large tidal prism coupled with limited sediment supply and the presence of fine sediments into which it incises. Spits formed by wind-driven sediment reworking of the shorelines fed the process of lagoonal segmentation. Multiple slumps, associated with these spits, have since filled the early depression in the subaerial unconformity. These were formed by margin instability associated with wave reworking of the lagoon and lacustrine shoreline during a period of drier climate in south-east Africa between 3700 and 2600 cal. BP. Consequently, lowered lake levels exposed more of the shoreline to wind-driven wave reworking and produced a more segmented waterbody. This was also coeval with an overall decrease in the depositional energy related to inlet closure, which resulted in the deposition of lacustrine fines and associated gyttja deposits. Back flooding of the back-barrier since produced a new inlet ~ 12 km to the north. The overall filling of the basin is controlled by along-strike changes to tidal effects (driven by segmentation and inlet relocation) in the absence of multiple marine sources and a diminished fluvial input. Such along-strike back flooding of incised valleys appears to be a peculiar attribute of coastal waterbodies of South Africa.

**References**

Allen, G.P., Posamentier, H.W., 1994 Transgressive facies and sequence architecture in mixed tide and wave-dominated incised valleys: example from the Gironde estuary, France. In: Dalrymple, R.W., Boyd, R., Zaitlin, B.A. (Eds.), Incised Valley Systems: Origin and Sedimentary Sequences. Society of Economic Palaeontologists and Mineralogists Special Publication 51, 226-240.

Benallack, K., Green, A.N., Humphries, M.S., Cooper, J.A.G., Dladla, N.N., Finch, J.M., 2016. The stratigraphic evolution of a large back-barrier lagoon system with a non-migrating barrier. Marine Geology 379, 64-77.

Botha, G.A., 2018. Lithostratigraphy of the late Cenozoic Maputaland Group. South African Journal of Geology 121, 95-108.

Botha, G.A., Porat, N., 2007. Soil chronosequence development in dunes on the southeast African coastal plain, Maputaland, South Africa. Quaternary International 162–163, 111–132.

Bortolin, E.C., Weschenfelder, J., Cooper, A., 2018. Incised valley paleoenvironments interpreted by seismic stratigraphic approach in Patos Lagoon, Southern Brazil. Brazilian Journal of Geology 48, 533-551.

Catuneanu, O., Abreu, V., Bhattacharya, J.P., Blum, M.D., Dalrymple, R.W., Eriksson, P.G., Fielding, C,R., Fisher, W.L., Galloway, W.E., Gibling, M.R., Giles, K.A., Holbrook, J.M., Jordan, R., Kendall, C.G.St.C., Macurda, B., Martinsen, O.J., Miall, A.D., Neal, J.E., Nummedal, D., Pomar, L., Posamentier, H.W., Pratt, B.R., Sarg, J.F., Shanley, K.W., Steel, R.J., Strasser, A., Tucker, M.E., Winker, C., 2009. Towards the standardization of sequence stratigraphy. Earth-Science Reviews 92, 1-33.

Cooper, J.A.G., Kilburn, R.N., Kyle, R., 1989. A Late Pleistocene molluscan assemblage from Lake Nhlange, Zululand, and its palaeoenvironment implications. South African Journal of Geology 92, 73-83.

Cooper, J.A.G., Green, A.N., Wright, C.I., 2012. Evolution of an incised valley coastal plain estuary under low sediment supply: a ‘give-up’ estuary. Sedimentology 59, 899-916.

Cooper, J.A.G., Green, A.N., and Loureiro, C., 2018a. Geological constraints on mesoscale coastal barrier behaviour. Global and Planetary Change 168, 15-34.

Cooper, J.A.G., Green, A.N., and Compton, J., 2018b. Sea-level change in southern Africa since the last glacial maximum. Quaternary Science Reviews 201, 303-318.

Chaumillon, E., Tessier, B., Reynaud, J-Y., 2010. Stratigraphic records and variability of incised valleys and estuaries along French coasts. Bulletin de la Societe Geologique de France 181, 75-85.

Davidson-Arnott, R., Conliffe Reid, H.E., 1994. Sedimentary processes and the evolution of the distal bayside of Long Point, Lake Erie. Canadian Journal of Earth Sciences 31, 1461-1473.

Davies, J.L., 1980. Geographic Variation in Coastal Development. Longman, New York. pp. 212.

De Lecea, A.M., Green, A.N., Strachan, K.L., Cooper, J.A.G., Wiles, E.A., 2017. Stepped Holocene sea-level rise and its influence on sedimentation in a large marine embayment: Maputo Bay, Mozambique. Estuarine, Coastal and Shelf Science 193, 25-36.

Dladla, N.N., Green, A.N., Cooper, J.A.G., Humphries, M.S., 2019. Geological inheritance and its role in the geomorphological and sedimentological evolution of bedrock-hosted incised valleys, lake St Lucia, South Africa. Estuarine, Coastal and Shelf Science 222, 154-167.

Dladla, N.N., Green, A.N., Cooper, J.A.G., Mehlhorn, P., Haberzettl, T., 2021. Bayhead delta evolution in the context of late Quaternary and Holocene sea-level change, Richards Bay, South Africa. Marine Geology 441, 106608.

Diab, R.D., Sokolic, F., 1996. Report on Wind and Wind Turbine Monitoring at Mabibi-Period September 1994 to February 1996. Department of Mineral and Energy Affairs Report, Pretoria. 8pp.

Du Preez, J.W., Wolmarans, L.G., 1986. Die geologie van die gebied Kosibaai. Explanation of sheet 2632. Geological Survey of South Africa.

Flemming, B.W., 1978. Underwater sand dunes along the southeast African continental shelf–Observations and implications. Marine Geology 26, 177-198.

Green, A.N., 2009. Palaeo-drainage, incised valley fills and transgressive systems tract sedimentation of the northern KwaZulu-Natal continental shelf, South Africa, SW Indian Ocean. Marine Geology 263, 46-63.

Green, A.N., 2011. The late Cretaceous to Holocene sequence stratigraphy of a sheared passive upper continental margin, northern KwaZulu-Natal, South Africa. Marine Geology 289, 17-28.

Green, A.N., Dladla, N., Garlick, G.L., 2013. Spatial and temporal variations in incised valley systems from the Durban continental shelf, KwaZulu-Natal, South Africa. Marine Geology 335, 148-161.

Green, A.N., Cooper, J.A.G., Wiles. E.A., De Lecea, A.M., 2015. Seismic architecture, stratigraphy and evolution of a subtropical marine embayment: Maphuto Bay, Mozambique. Marine Geology 369, 300-309.

Green, A.N., Humphries, M.S., Cooper, J.A.G., Strachan, M., Gomes, M., Dladla, N.N., 2022a. The Holocene evolution of Lake St Lucia, Africa's largest estuary: Geological implications for contemporary management. Estuarine, Coastal and Shelf Science 266, 107745.

Green, A.N., Flemming, B.W., Cooper, J.A.G., Wanda, T.F., 2022b. Bedform evolution and dynamics of a geostrophic current-swept shelf, northern KwaZulu-Natal, South Africa. Geo-Marine Letters 42, 1.

Hayes, M.O., 1979. Barrier island morphology as a function of tidal and wave regime. In: Leatherman, S.P. (Ed.), Barrier Islands from the Gulf of Mexico. Academic Press, New York. pp. 1-29.

Hill, B.J., 1975. The origin of Southern African coastal lakes. Transactions of the Royal Society of South Africa 41, 225-240.

Hogg, A.G., Hua, Q., Blackwell, P.G., Niu, M., Buck, C.E., Guilderson, T.P., Heathon, T.J., Palmer, J.G., Reimer, P.J., Reimer, R.W., Turney, C.S.M., Zimmerman, S.R.H. 2013. SHCal13 southern hemisphere calibration, 0-50,000 years cal BP. Radiocarbon 55, 1889-1903.

Humphries, M.S., Green, A.N., Finch, J.M., 2016. Evidence of El Niño driven desiccation cycles in a shallow estuarine lake: The evolution and fate of Africa's largest estuarine system, Lake St Lucia. Global and Planetary Change 147, 97-105.

Humphries, M.S., Kirsten, K.L., McCarthy, T.S., 2019. Rapid changes in the hydroclimate of southeast Africa mid- to late-Holocene. Quaternary Science Reviews 212, 178-186.

Humphries, M., Green, A., Higgs, C., Strachan, K., Hahn, A., Pillay, L., Zabel, M., 2020. High-resolution geochemical records of extreme drought in southeastern Africa during the past 7000 years. Quaternary Science Reviews 236, 106294.

Journal Pre-proof

Jackson, D.W.T., Cooper, J.A.G., Green, A.N., 2014. A preliminary classification of coastal sand dunes of KwaZulu-Natal. Journal of Coastal Research 70, 718-722.

Lutjeharms, J.R.E., 2006. The ocean environment off south-eastern Africa: a review. South African Journal of Science 102, 419–426.

Mallinson, D., Culver, S., Leorri, E., Mitra, S., Mulligan, R., Riggs, S., 2018. Barrier Island and Estuary Co-evolution in Response to Holocene Climate and Sea-Level Change: Pamlico Sound and the Outer Banks Barrier Islands, North Carolina, USA. In: Moore, L., Murray A. (Eds.), Barrier Dynamics and Response to Changing Climate. Springer, Cham. pp. 91-120.

Mattheus, C.R., Rodriguez, A.B., 2011. Controls on late Quaternary incised-valley dimension along passive margins evaluated using empirical data. Sedimentology 58, 1113-1137.

Miner, M.D., Kulp, M.A., Fitzgerald, D.M., 2007. Tidal Versus Shoreface Ravinement and Tidal Inlet Fill Preservation Potential for Transgressive Tidal Inlets, Mississippi River Delta Plain, U.S.A. Journal of Coastal Research 50, 805-809.

Mitchum, R.M., Vail, P.R., 1977. Seismic stratigraphy and global changes of sea level, part 7: seismic stratigraphy interpretation procedure. In: Payton C.E. (Ed.), Seismic Stratigraphy-Applications to Hydrocarbon Exploration. American Association of Petroleum Geologists Memoir 26, 135-143.

Moran, K.L., Mallinson, D.J., Culver, S.J., Mulligan, R.P., 2015. Late Holocene Evolution of Currituck Sound, North Carolina, USA: Environmental Change Driven by Sea-Level rise, Storms, and Barrier Island Morphology. Journal of Coastal Research 31, 827-841.

Ndlovu, M., Demlie, M., 2016. Hydrogeological characterization of the Kosi Bay Lakes system, north-eastern South Africa. Environmental Earth Sciences 75, 1334.

Nichols, M.M., 1989. Sediment accumulation rates and relative sea-level rise in lagoons. Marine Geology 88, 201-219.

Nutz, A., Schuster, M., Ghienne, J.-F., Roquin, C., Hay, M.B., Retif, F., Certain, R., Robin, N., Raynal, O., Cousineau, P.A., Team, S., Bouchette, F., 2015. Wind-driven bottom currents and related sedimentary bodies in Lake Saint-Jean (Québec, Canada). Geological Society of America Bulletin 127, 1194-1208.

Orme, A.R., 1973. Barrier and lagoon systems along the Zululand coast, South Africa. In: Coates, D.R. (ed.), Coastal Geomorphology. New York State University, Binghamton, pp. 181-217.

Ramsay, P.J., Cooper, J.A.G., 2002. Late Quaternary sea-level change in South Africa. Quaternary Research 57, 82-90.

Riggs, S.R., Ames, D.V., Culver, S.J., Mallinson, D.J., Corbett, D.R., Walsh, J.P., 2009. In the eye of a human hurricane: Oregon Inlet, Pea Island, and the northern Outer Banks of North Carolina. In: Kelley, J.T., Young, R.S., Pilkey, O.H. (Eds.), Identifying America's most vulnerable oceanfront communities: a geological perspective. Geological Society of America, Special Publication, Boulder, CO. pp. 43-72.

Rossouw, J., 1984. Review of existing wave data, wave climate and design waves for South Africa and West African (Namibian) coastal waters. Coastal Engineering and Hydraulics, National Research Institute for Oceanology, CSIR Report T/SEA 8401, Stellenbosch, 61 pp.

Roy, P.S., 1984. New South Wales Estuaries: their origin and evolution. In: Thom, B.G. (Ed.), Coastal Geomorphology in Australia. Academic Press, Sydney, Australia, pp. 99-121.

Rucińska- Zjadacz, M., Wróblewski, R., 2018. The complex geomorphology of a barrier spit progradng into deep water, Hell Peninsula, Poland. Geo-Marine Letters 38, 513-525.

Scasso, R.A., Cuitiño, J.I., 2016. Sequential development of tidal ravinement surfaces in macro- to hypertidal estuaries with high volcaniclastic input: the Miocene Puerto Madryn Formation (Patagonia, Argentina). Geo-Marine Letters 37, 427-440.

South African Navy., 2009. Tide Tables. South African Navy, Simonstown.

Simms, A.R., Aryal, N., Miller, L., Yokoyama, Y., 2010. The incised valley of Baffin Bay, Texas: a tale of two climates. Sedimentology 57, 642-669.

Tessier, B., 2012. Stratigraphy of tide-dominated estuaries. In: Davies R.A. (Eds.), Principles of tidal sedimentology. Springer, Heidelberg. pp. 109-128.

Van Heerden, I.L., Swart, D.H., 1986. An assessment of past and present geomorphological and sedimentary process operative in the St. Lucia estuary and environs. Marine Geoscience and Sediment Dynamics Division, National Institute for Oceanology, CSIR Research Report No. 569.

Weschenfelder, J., Klein, A.H., Green, A.N., Aliotta, S., de Mahiques, M.M., Neto, A.A., Terra, L.C., Corrêa, I.C., Calliari, L.J., Montoya, I., Ginsberg, S.S., 2016. The control of palaeotopography in the preservation of shallow gas accumulation: examples from Brazil, Argentina and South Africa. Estuarine, Coastal and Shelf Science 172, 93-107.

Wright, C.I., 1995. A Reconnaissance study of the Zululand coastal plain dune cordon chronology. Council for Geoscience, Report No. 1995-0132, 12p.

Wright, C.I., 1999. The Cenozoic evolution of the Northern KwaZulu-Natal coastal plain. Unpublished PhD thesis, Department pf Geology and Computer Science, University of Natal, Durban. 243pp.

Wright, C.I., Lindsay, P., Cooper, J.A.G., 1997. The effect of sedimentary processes on the ecology of the mangrove fringed Kosi estuary/lake system, South Africa. Mangroves Salt Marshes 1, 79-94.

Wright, C.I., Cooper, J.A.G., Kilburn, R.N., 1999. Mid Holocene Palaeoenvironments from Lake Nhlange, Northern KwaZulu-Natal, South Africa. Journal of Coastal Research 15, 991-1001.

Wright, C.I., Miller, W.R., Cooper, J.A.G., 2000. The late Cenozoic evolution of coastal water bodies in Northern KwaZulu-Natal, South Africa. Marine Geology 167, 207-229.

Zaitlin, B.A., Dalrymple, R.W., Boyd, R., 1994. The stratigraphic organization of incised-valley systems associated with relative sea level change. In: Dalrymple, R.W., Boyd, R., Zaitlin, B.A. (Eds.), Incised Valley Systems: Origin and Sedimentary Sequences. Society of Economic Palaeontologists and Mineralogists Special Publication 51, 45-60.

Zaremba, N., Mallinson, D.J., Leorri, E., Culver, S., Riggs, S., Mulligan, R., Horsman, E., Mitra, S., 2016. Controls on the stratigraphic framework and paleoenvironmental change within a Holocene estuarine system: Pamlico Sound, North Carolina, USA. Marine Geology 379, 109-123.

Zecchin, M., Catuneanu, O., 2013. High-resolution sequence stratigraphy of clastic shelves I: Units and bounding surfaces. Marine and Petroleum Geology 39, 1-25.

Zenkovich, V.P., 1959. On the genesis of cuspate spits along lagoon shore. Journal of Geology. 67, 269-277.

**Figure and table captions**

**Fig. 1.** (a) Locality map of the study area, showing the four interconnected lakes of Kosi Bay. Note the positions of Core KB2 and 4 in Lake Mpungwini and Lake Amanzimnyama, as well as the location of the seismic track lines. (b) Sea level fluctuations since ~ 10000 Cal. BP (c). Shows the location of the study area on the north-eastern South African coastline.

**Fig. 2.** (a) WNW-ESE seismic reflection profile (from Lake Mpungwini) displaying interpreted (top) and raw (bottom) seismic data. Only Units A, C2, D and E are evident in this profile. Note the position of Core KB2. (b) WNW-ESE seismic reflection profile (from Lake Mpungwini) displaying interpreted (top) and bottom (raw) seismic data. Note the incisions formed in Surface SB. Only Units A, B, C1 and E are present.

**Fig. 3.** NW-SE seismic reflection profile (From Lake Nhlange) displaying interpreted (top) and raw (bottom) seismic data. Only Unit D is absent from this seismic line. Note the presence of both Surfaces SB and T-RS. The enlarged seismic data show the prograding spits (Unit C1) and prograding marginal spits (Unit C2).

**Fig. 4.** NNE-SSW seismic reflection profile (From Lake Nhlange) displaying interpreted (top) and raw (bottom) seismic data. Only Unit C1 is absent from this seismic line. Note the presence of both Surfaces SB and T-RS. The enlarged seismic data show Unit D (Fig. 4a) and Unit C2.

**Fig. 5.** NW-SE seismic reflection profile (from Lake Nhlange) displaying interpreted (top) and raw (bottom) seismic data. Only Units A, B and E are present on this seismic line. The enlarged seismic data show numerous incisions in Surface SB, as well as minor incisions in Surface T-RS.

**Fig. 6.** NNW-SSE seismic reflection profile (from Lake Nhlange) displaying interpreted (top) and raw (bottom) seismic data. Unit C2 and D are absent from this line. Note the laterally extensive Surfaces SB and T-RS. The enlarged seismic data show broad incised valleys formed in Surface SB onlapped by prograding spits (Unit C1). Note the broad U-shaped incised valley.



**Fig. 7.** NW-SE seismic reflection profile (from Lake Nhlange) displaying interpreted (top) and raw (bottom) seismic data. Only Unit A, B and E are present on this seismic line. The enlarged seismic data depict the thick central basin deposits (Unit B) that fill the incisions in SB.

**Fig. 8.** (a) WNW-ESE seismic reflection profile (from Lake Nhlange) displaying interpreted (top) and raw (bottom) seismic data. Only Unit C1 and Surface T-RS are absent from this seismic line. The enlarged seismic data show an example of a slumped prograding marginal spit. (b) W-E seismic reflection profile (from Lake Nhlange) displaying interpreted (top) and raw (bottom) seismic data. Unit B and C1, and Surface T-RS are absent from this seismic line. The enlarged seismic data show a prograded marginal spit that has slumped into the main depocentre.

**Fig. 9. S**unshaded relief surface of the (a) the SB unconformity, (b) T-RS unconformity and (c) contemporary bathymetry, as well as isopachs of the (d) post SB and (e) SB to T-RS sediment distribution. Note the inheritance of the main incision into SB by T-RS and later the bathymetry.

**Fig. 10.** (a) Sedimentology and geochronology of Core KB2 (from Lake Mpungwini). Note the AMS $C^{14}$ dates, the mean grain sizes (2) and the sorting (3) and skewness (4) coefficients. (b) Sedimentology of Core KB4 (from Lake Amanzimnyama). Note the AMS $C^{14}$ dates, the mean grain sizes (2) and the sorting (3) and skewness (4) coefficients.

**Fig. 11.** Previous cores collected from Lake Nhlange (modified from Wright et al. (1999). Figs. 11a, b and c correspond to Cores 1, 3 and 5 respectively. Note the recalibrated $C^{14}$ date for Core 3 (Fig. 11b)

**Fig. 12.** Comparison in shape of the incised valleys formed in unconsolidated sediments from (a) the Cape Hatteras region of North Carolina (modified from Zaremba et al., 2016), (b) the northern Gulf of Mexico (modified Mattheus and Rodriguez, 2011) and (c) this study.

**Fig. 13.** The schematic evolution of the Kosi Bay system's stratigraphy. (a) LGM-age incision into unconsolidated Kosi Bay Formation sediments. (b) Post-LGM partial infilling of the incised valleys, development of wind-driven spits signifying early stages of lagoonal segmentation. (c) tidal scouring (forming T-RS), continued segmentation, onset of lacustrine conditions in Lake Amanzimnyama, closure of the Bhanga Nek inlet. (d) Development of prograding marginal spits and eventual slumping, deposition of lacustrine fines, development of the modern tidal-inlet.

**Table 1.** AMS radiocarbon ages from this study, and previous $C^{14}$ dates from Wright et al. (1999) calibrated using the Southern Hemisphere atmospheric curve SHCal13.

**Table 2.** A simplified stratigraphic framework for the Kosi Bay system, describing seismic units, the age of each unit, and the interpreted depositional environments.

| Location | Core sample | Depth (m) | Material | $C^{14}$ age (yr BP) | Age (cal. BP) |
|---|---|---|---|---|---|
| Lake Mpungwini | KB2-40 | 0.40 | Organic sediment | 490 ± 30 | 510 ± 20 |
| Lake Mpungwini | KB2-352 | 3.52 | Plant material | 1250 ± 30 | 1120 ± 30 |
| Lake Mpungwini | KB2-734 | 7.34 | Organic sediment | 2890 ± 30 | 2965 ± 30 |
| Lake Amanzimnyama | KB4-150 | 1.5 | Organic sediment | 900 ± 30 | 760 ± 30 |
| Lake Amanzimnyama | KB4-550 | 5.5 | Organic sediment | 2920 ± 30 | 2980 ± 100 |
| Lake Amanzimnyama | KB4-902 | 9.02 | Organic sediment | 3990 ± 30 | 4370 ± 85 |
| Lake Nhlange | Core 2 CAR-1368 | 1.32 | Shell | 3020 ± 70 | 3160 ± 200 |
| Lake Nhlange | Core 3 CAR-1370 | 2.3 | Shell | 2780 ± 80 | 2900 ± 165 |
| Lake Nhlange | Core 4 CAR-5420 | 165 | Shell | 5420 ± 80 | 6150 ± 160 |
| Kosi mouth | Pta-4972 | - | Coral (*Favites*) | 1610 ± 70 | 1450 ± 140 |

| Underlying surface | Seismic unit/surface | Sub-unit | Modern description | Thickness | Characteristics | Interpreted depositional environment | Age |
|---|---|---|---|---|---|---|---|
| T-RS? | E | N/A | Capping fill | 1.8-9 m | Laterally extensive, low amplitude, aggrading, draped reflections. May be overlain by a thin (1-2 m) layer of acoustically transparent material. | Lacustrine fines | Holocene |
| | D | N/A | Prograding wedge | ≥ 10 m | Steeply dipping, chaotic, high amplitude, oblique-parallel to sigmoidal reflectors that can merge upslope with Unit C. | Slump deposit | Holocene |
| T-RS | C | C2 | | ≥ 10 m | Steeply dipping, prograding, moderate to high amplitude reflectors. Progrades into the basin from the margins of the system. | Prograding marginal spit | Holocene |
| | T-RS | N/A | Extensive erosional surface | | Laterally extensive reflector, characterised by numerous incisions of various depths. | Tidal ravinement surface | Holocene |

| | | | | | | | |
|---|---|---|---|---|---|---|---|
| | C | C1 | | $\leq$ 6 m | Steeply dipping, prograding, moderate to high amplitude refelctors. Progrades into basin from channels and valley interfluves of SB. | Prograding sand spit | Late Pleistocene/Holocene? |
| SB | B | N/A | Well-developed draped package (valley fill) | Average: 10-18 m | Thickly developed. Concave upwards, aggrading reflectors of moderate low amplitude. | Central basin deposits | Late Pleistocene/Holocene |
| | SB | N/A | | | Undulating surface. Erosionally truncates Unit A and forms numerous incised valleys. | | Late Pleistocene |
| | A | N/A | Acoustic basement | >50 m | discontinuous and chaotic, moderate amplitude reflectors with no particular reflection configuration. Randomly dipping in different directions. | Last Glacial Maximum | Mid to late Pleistocene |

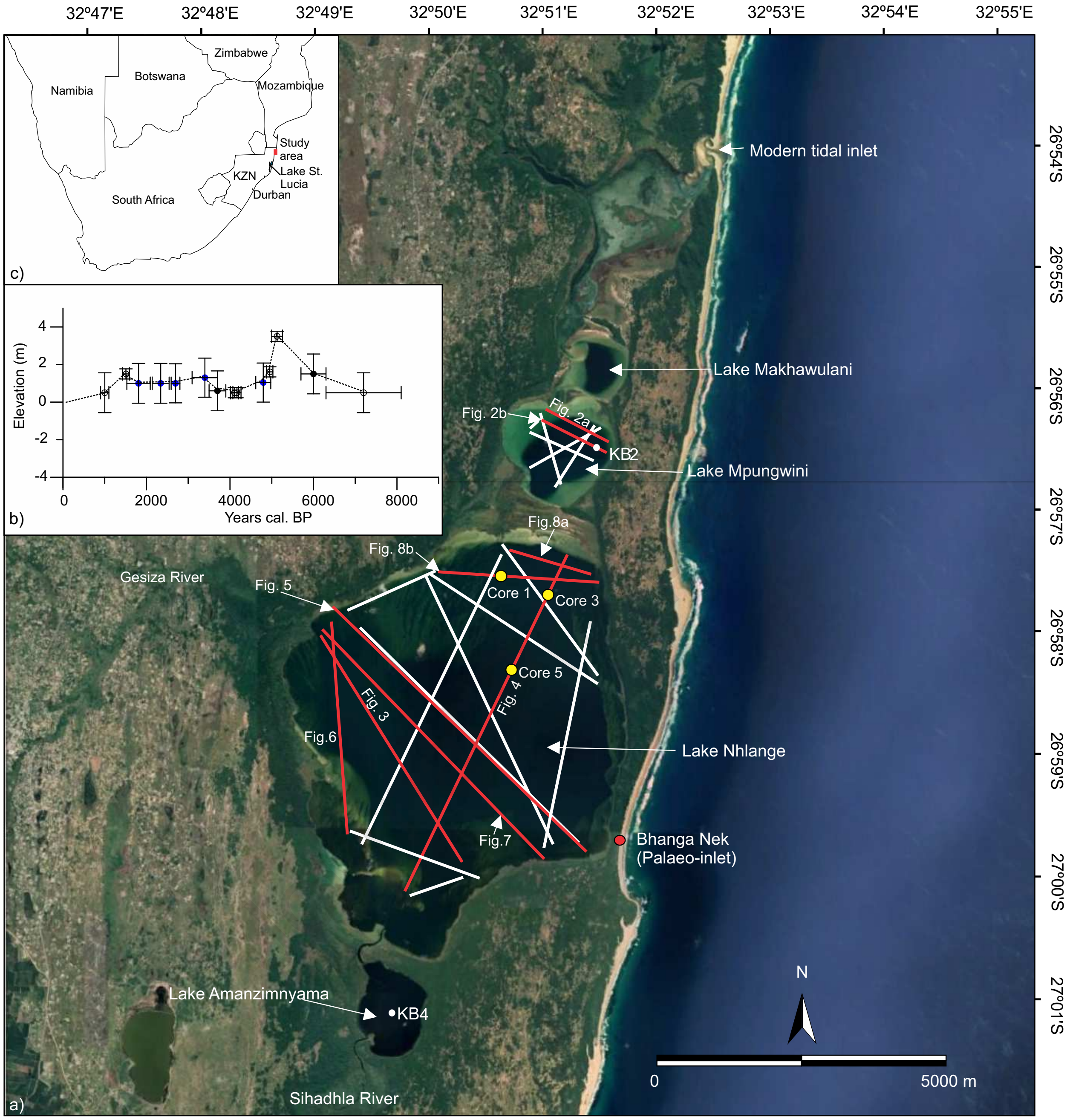
32°47'E
32°48'E
32°49'E
32°50'E
32°51'E
32°52'E
32°53'E
32°54'E
32°55'E
26°54'S
26°55'S
26°56'S
26°57'S
26°58'S
26°59'S
27°00'S
27°01'S
Zimbabwe
Botswana
Namibia
Mozambique
Study area
Lake St. Lucia
KZN
Durban
South Africa
c)
Elevation (m)
4
2
0
-2
-4
0
2000
4000
6000
8000
Years cal. BP
b)
Modern tidal inlet
Lake Makhawulani
Fig. 2b
Fig. 2a
KB2
Lake Mpungwini
Fig.8a
Fig. 8b
Gesiza River
Fig. 5
Core 1
Core 3
Core 5
Fig. 3
Fig. 4
Fig.6
Lake Nhlange
Fig.7
Bhanga Nek
(Palaeo-inlet)
N
Lake Amanzimnyama
KB4
0
5000 m
Sihadhla River
a)

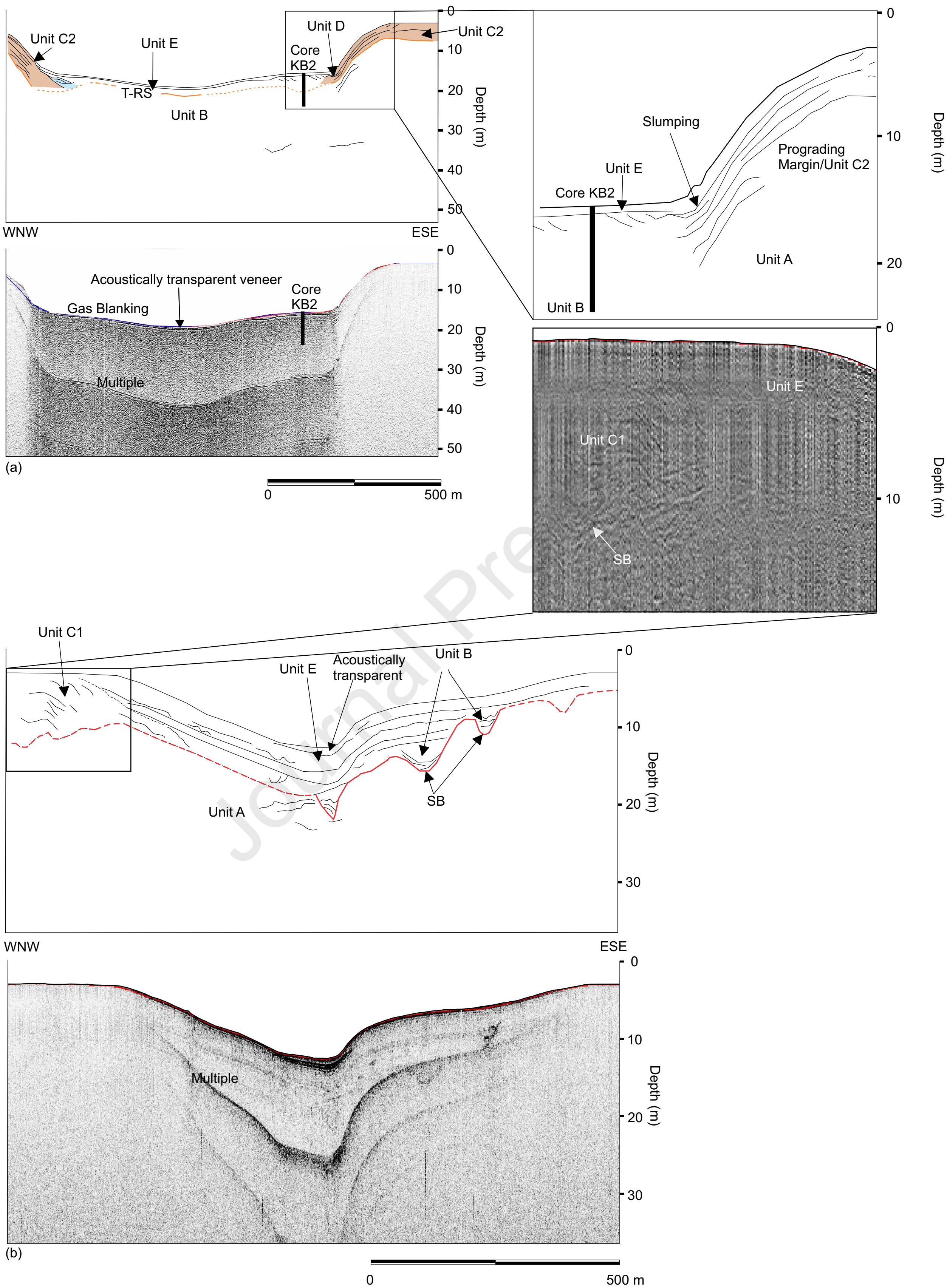
Unit C2
Unit E
Unit D
Core KB2
Unit C2
T-RS
Unit B
WNW
ESE
Depth (m)
Acoustically transparent veneer
Gas Blanking
Core KB2
Multiple
(a)
0
500 m
Slumping
Unit E
Core KB2
Prograding Margin/Unit C2
Unit A
Unit B
Unit E
Unit C1
SB
Unit C1
Unit E
Acoustically transparent
Unit B
Unit A
SB
WNW
ESE
Multiple
(b)
0
500 m

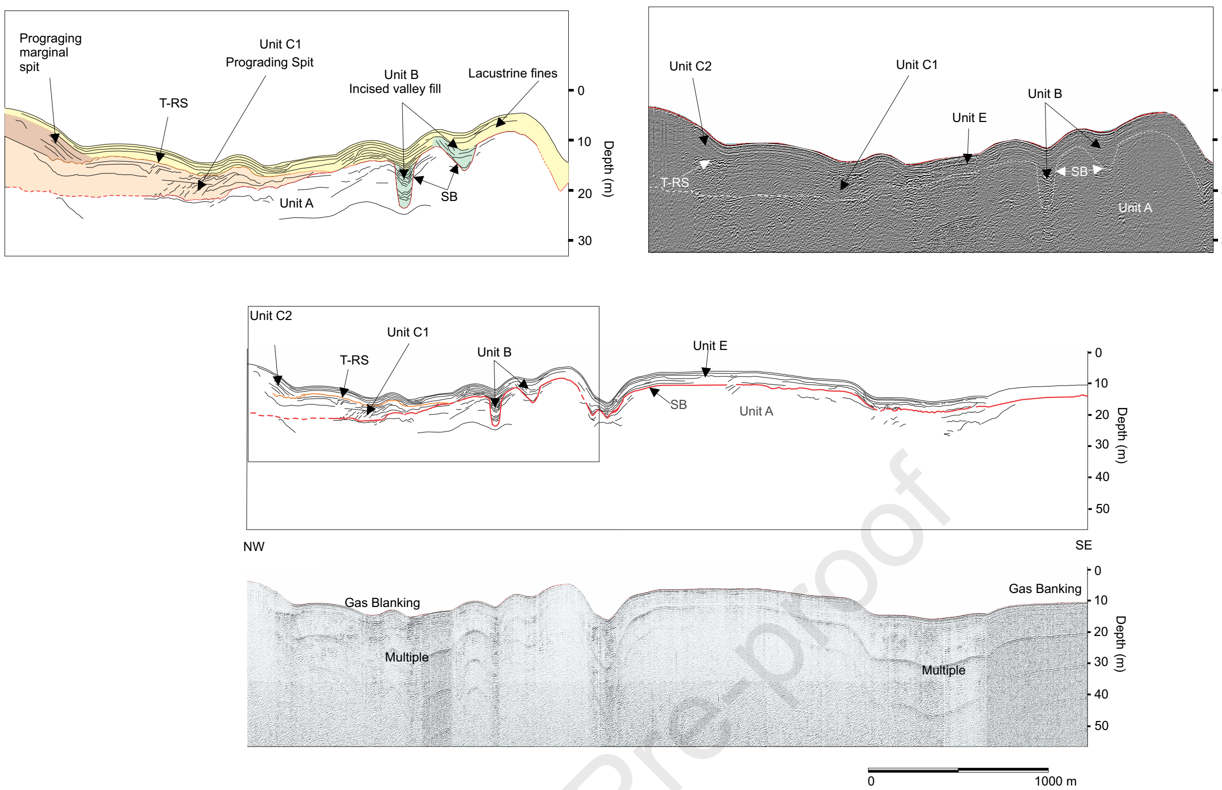
Prograging marginal spit
Unit C1
Prograding Spit
Unit B
Incised valley fill
Lacustrine fines
T-RS
Unit A
SB
Depth (m)
Unit C2
Unit E
Unit A
NW
SE
Gas Blanking
Multiple
Gas Banking
0
1000 m

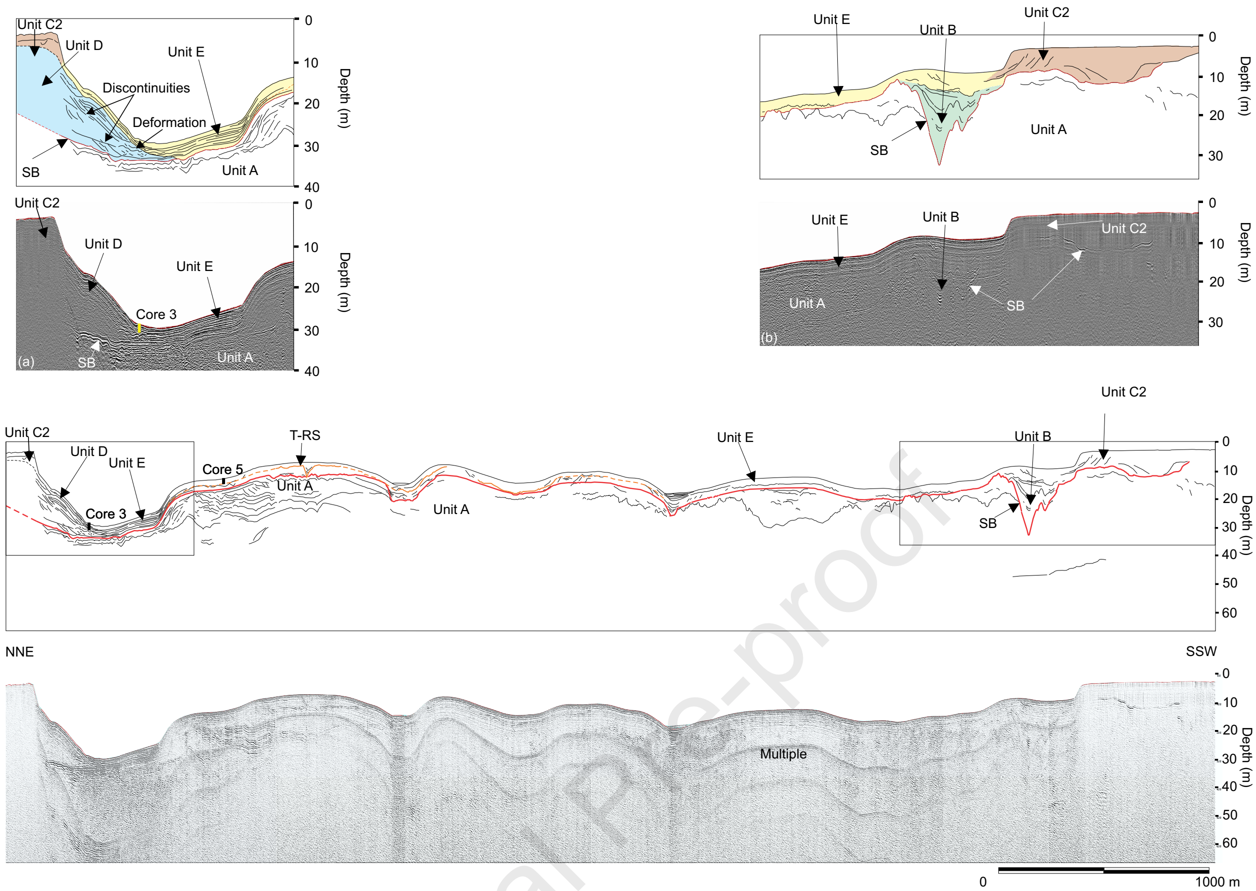
Unit C2
Unit D
Unit E
Discontinuities
Deformation
SB
Unit A
Depth (m)
0
10
20
30
40
Core 3
(a)
Unit B
(b)
T-RS
Core 5
50
60
NNE
SSW
Multiple
1000 m

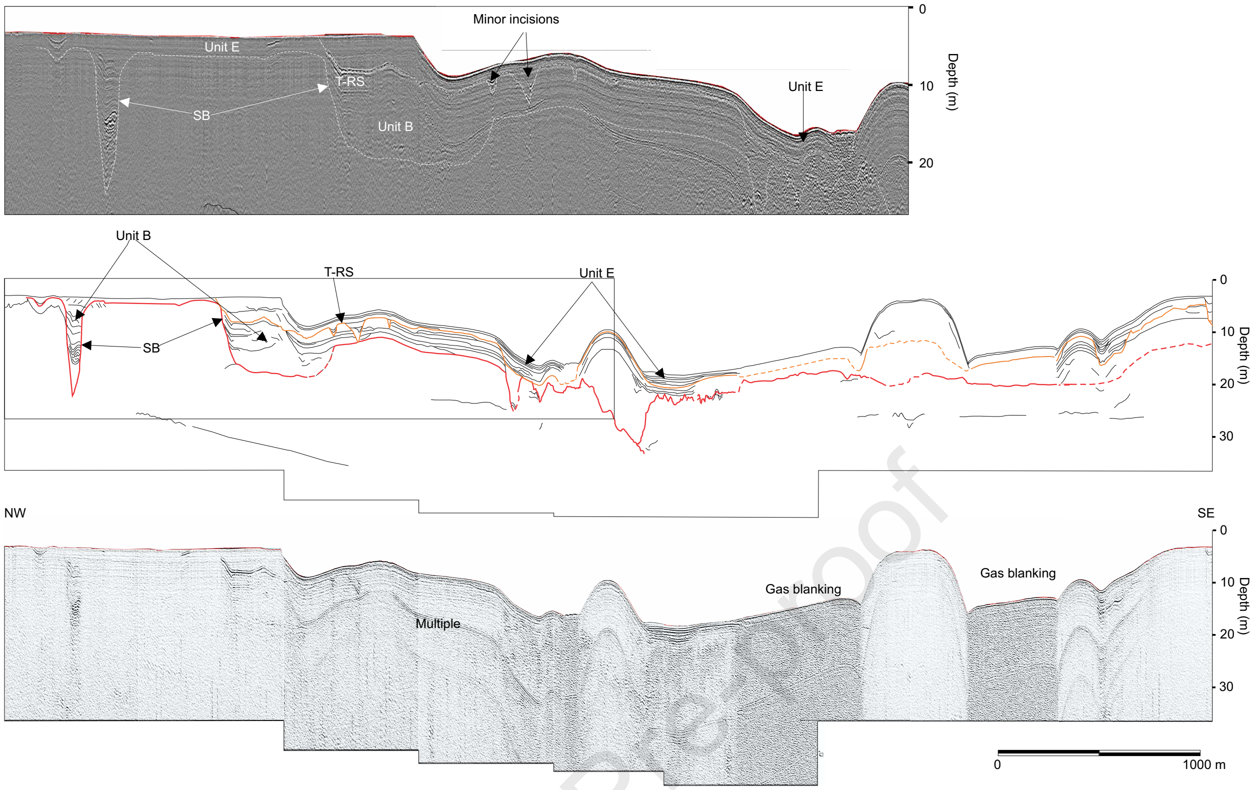

Minor incisions
Unit E
T-RS
SB
Unit B
Unit E
Depth (m)
0
10
20
Unit B
T-RS
Unit E
SB
0
10
20
30
Depth (m)
NW
SE
Gas blanking
Gas blanking
Multiple
0
10
20
30
Depth (m)
0
1000 m

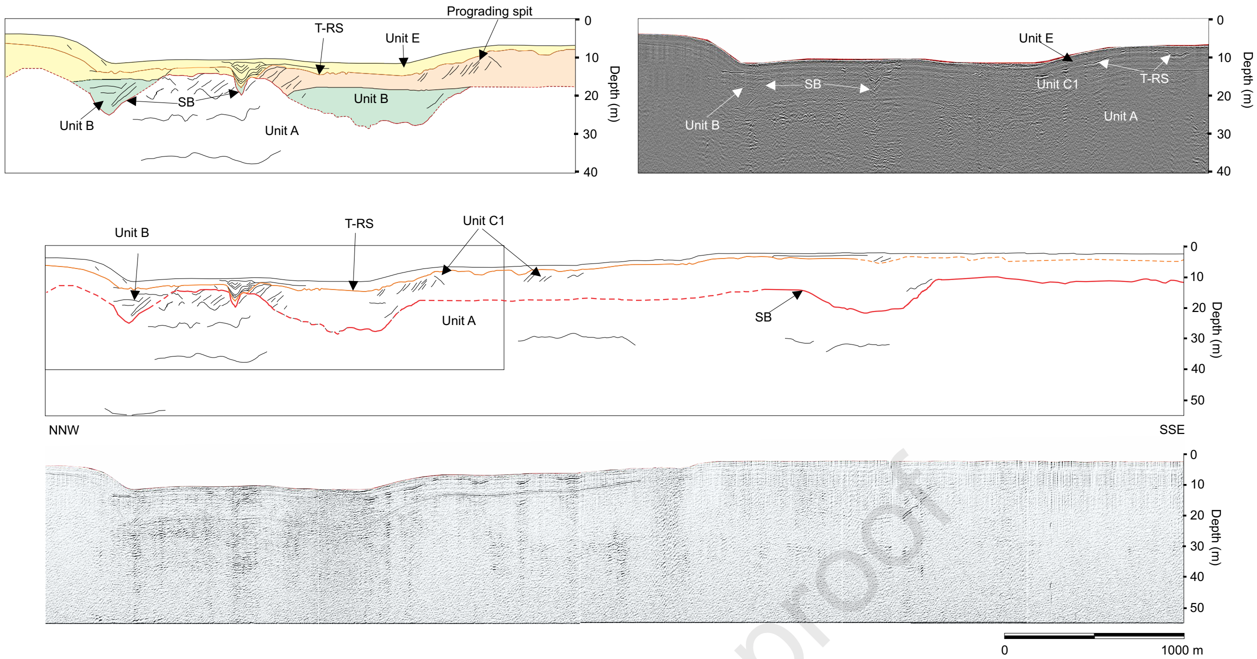

Prograding spit
T-RS
Unit E
Unit B
SB
Unit B
Unit A
Depth (m)
0
10
20
30
40
Unit E
SB
Unit C1
T-RS
Unit A
Unit B
Unit B
T-RS
Unit C1
Unit A
SB
50
NNW
SSE
0
1000 m

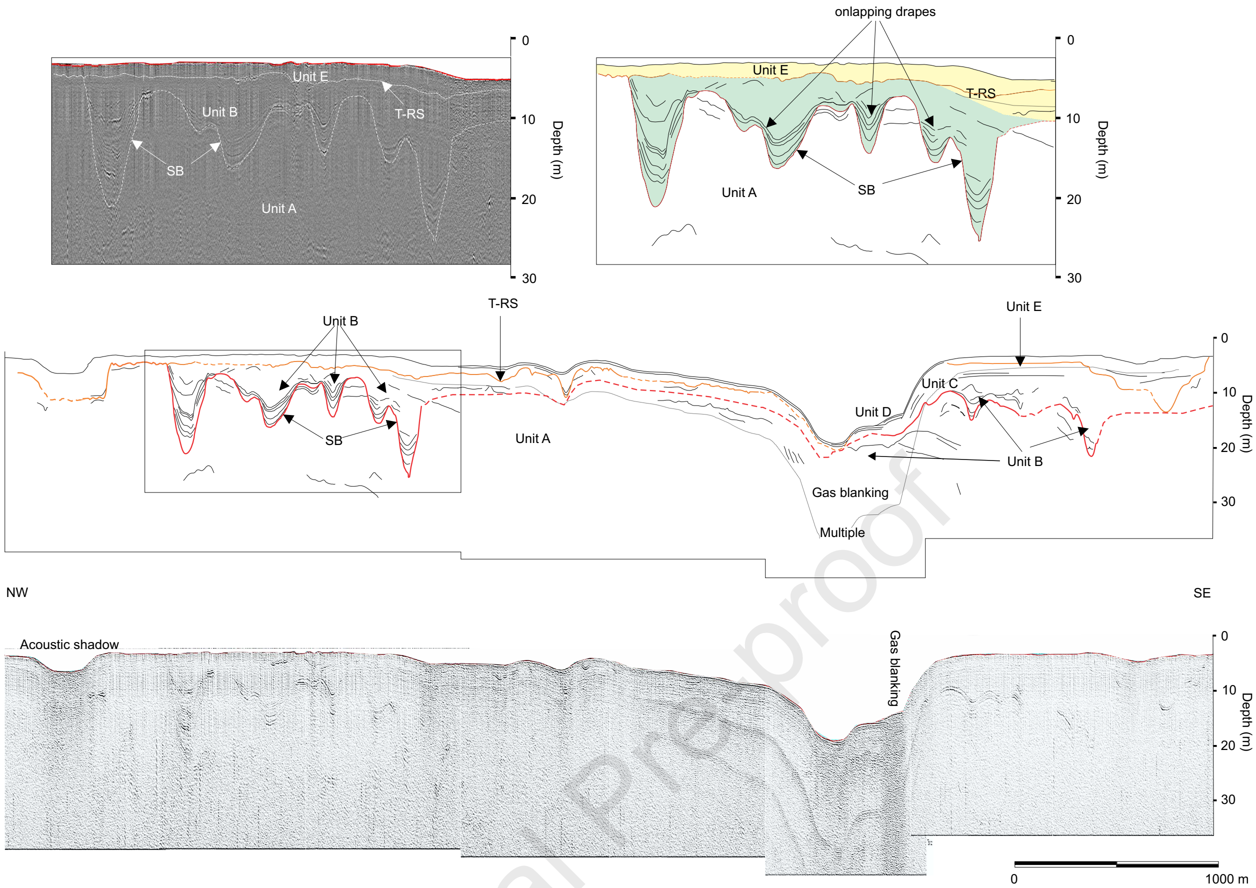
Unit E
Unit B
T-RS
SB
Unit A
Depth (m)
0
10
20
30
onlapping drapes
Unit E
T-RS
Unit A
SB
Depth (m)
Unit B
T-RS
Unit E
Unit C
Unit D
SB
Unit A
Unit B
Gas blanking
Multiple
NW
SE
Acoustic shadow
Gas blanking
0
1000 m

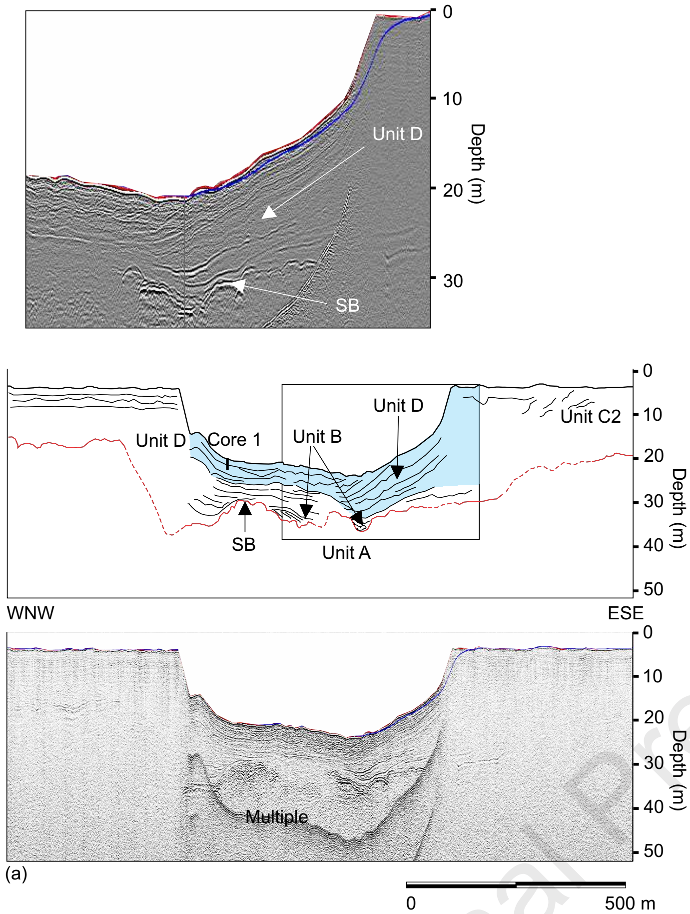

Unit D
SB
Depth (m)
0
10
20
30
Unit D
Core 1
Unit B
Unit D
Unit C2
SB
Unit A
0
10
20
30
40
50
WNW
ESE
Multiple
(a)
0
500 m


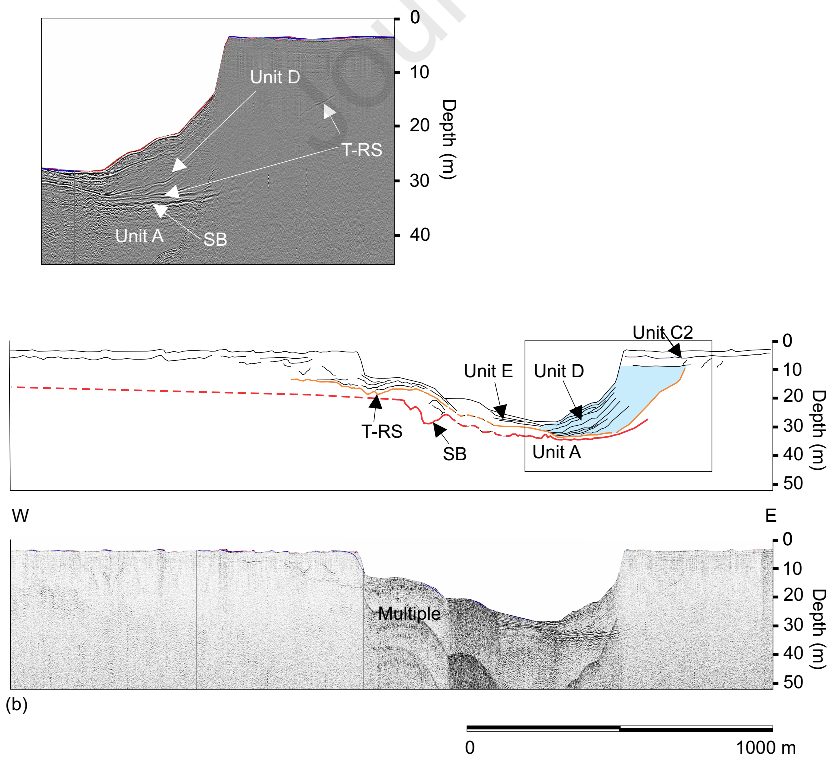

Unit D
T-RS
Unit A
SB
Depth (m)
0
10
20
30
40
Unit C2
Unit E
Unit D
T-RS
SB
Unit A
50
W
E
Multiple
(b)
0
1000 m

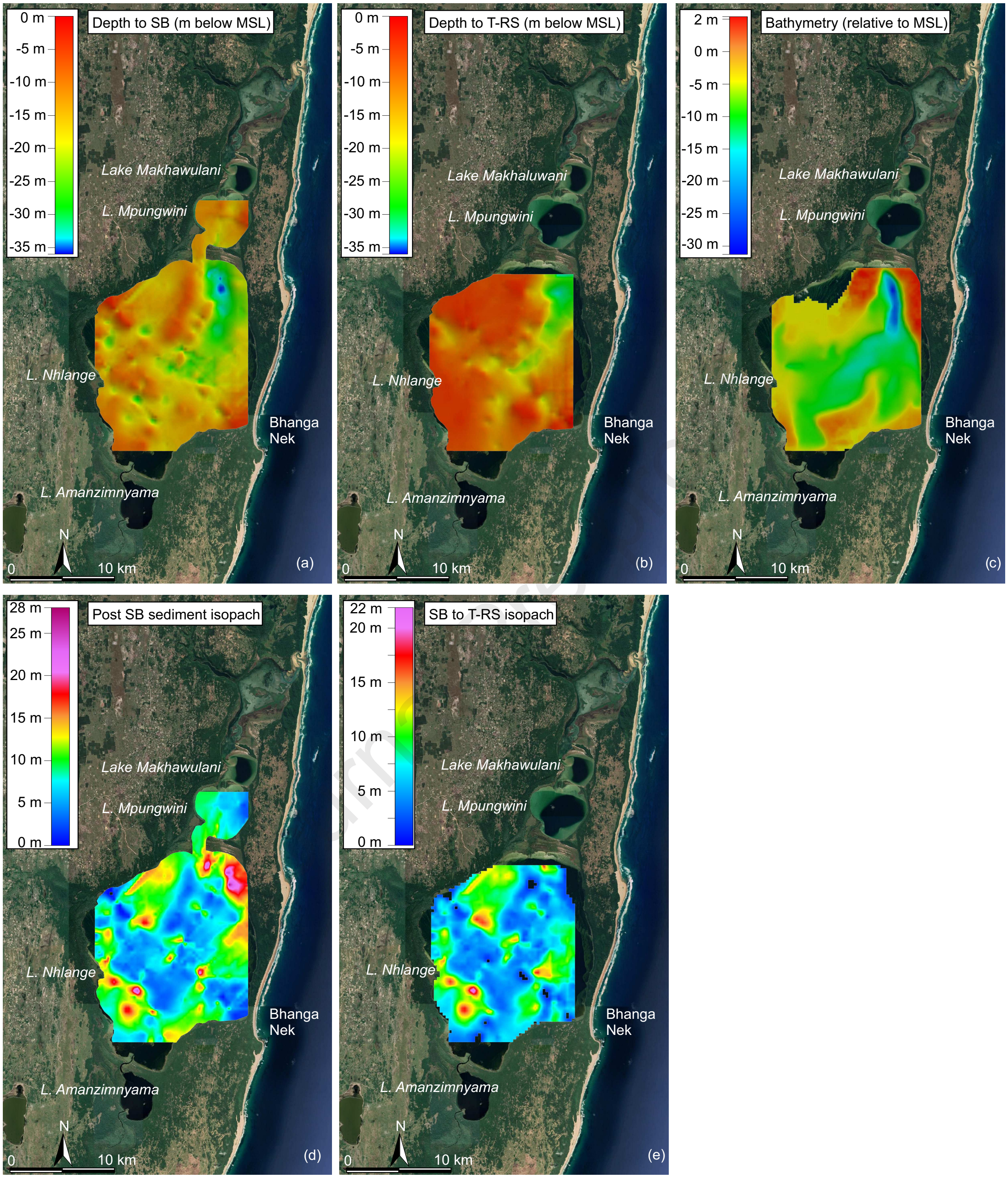
0 m
-5 m
-10 m
-15 m
-20 m
-25 m
-30 m
-35 m
Depth to SB (m below MSL)
Lake Makhawulani
L. Mpungwini
L. Nhlange
Bhanga Nek
L. Amanzimnyama
N
0
10 km
(a)
Depth to T-RS (m below MSL)
Lake Makhaluwani
(b)
2 m
Bathymetry (relative to MSL)
(c)
28 m
25 m
20 m
15 m
10 m
5 m
Post SB sediment isopach
(d)
22 m
SB to T-RS isopach
(e)

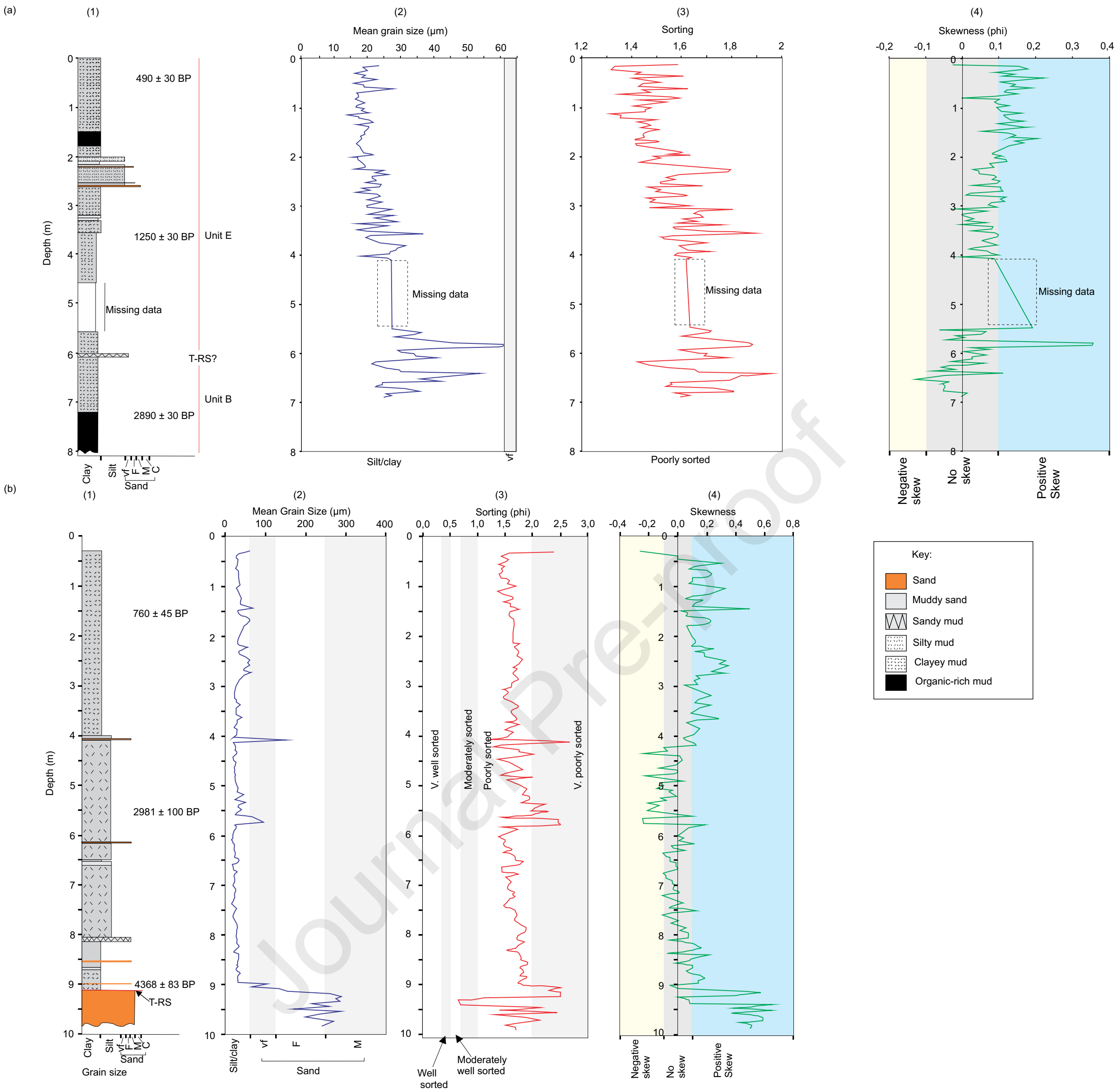
(a)
(1)
(2)
(3)
(4)
Mean grain size (µm)
Sorting
Skewness (phi)
490 ± 30 BP
1250 ± 30 BP
Unit E
Missing data
T-RS?
Unit B
2890 ± 30 BP
Depth (m)
Clay
Silt
vf
F
M
C
Sand
Silt/clay
Poorly sorted
Negative skew
No skew
Positive Skew
(b)
Mean Grain Size (µm)
Sorting (phi)
Skewness
760 ± 45 BP
2981 ± 100 BP
4368 ± 83 BP
T-RS
Grain size
V. well sorted
Moderately sorted
Poorly sorted
V. poorly sorted
Well sorted
Moderately well sorted
Key:
Sand
Muddy sand
Sandy mud
Silty mud
Clayey mud
Organic-rich mud

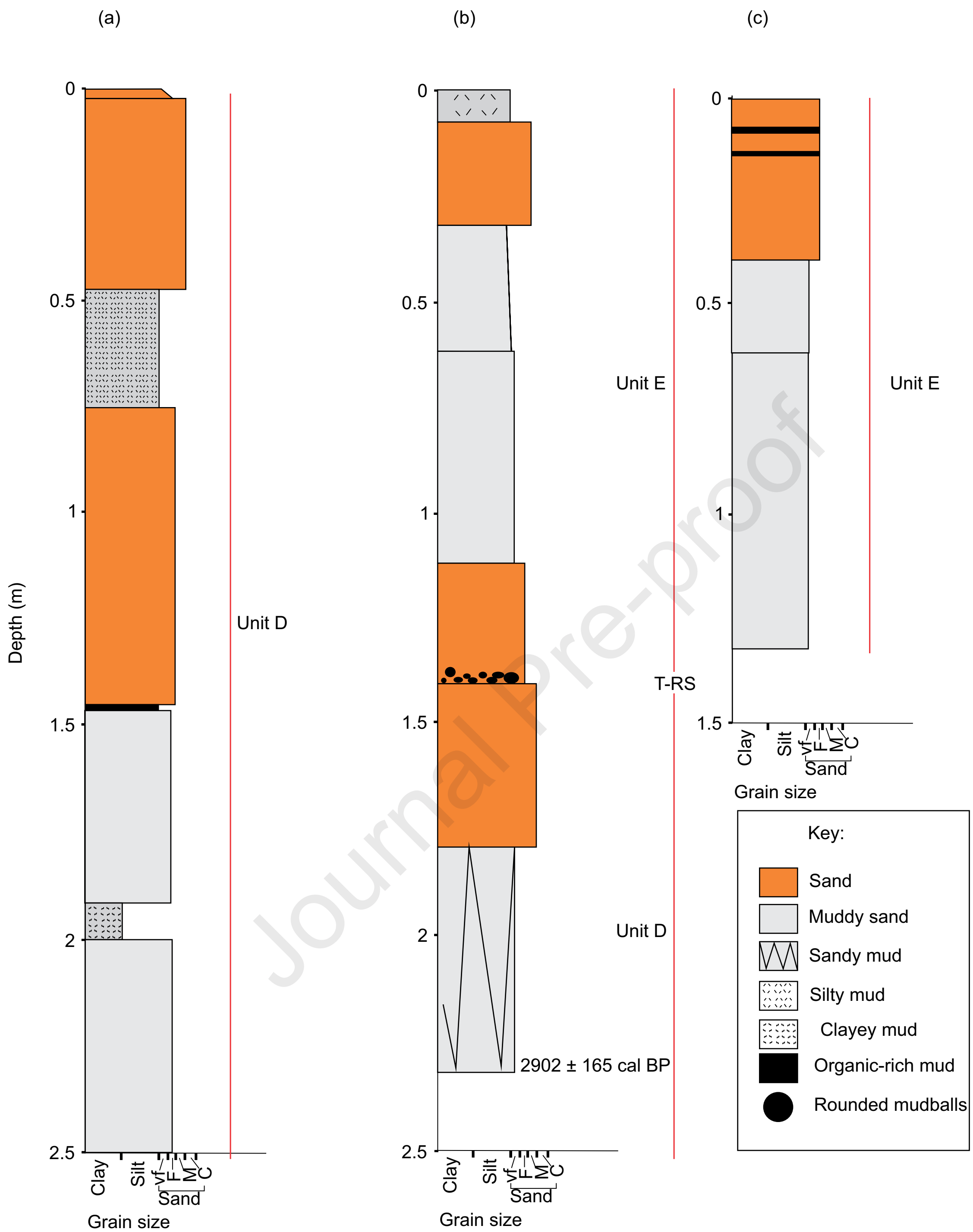
(a)
(b)
(c)
Depth (m)
0
0.5
1
1.5
2
2.5
Unit D
Unit E
T-RS
2902 ± 165 cal BP
Clay
Silt
vf
F
M
C
Sand
Grain size
Key:
Sand
Muddy sand
Sandy mud
Silty mud
Clayey mud
Organic-rich mud
Rounded mudballs

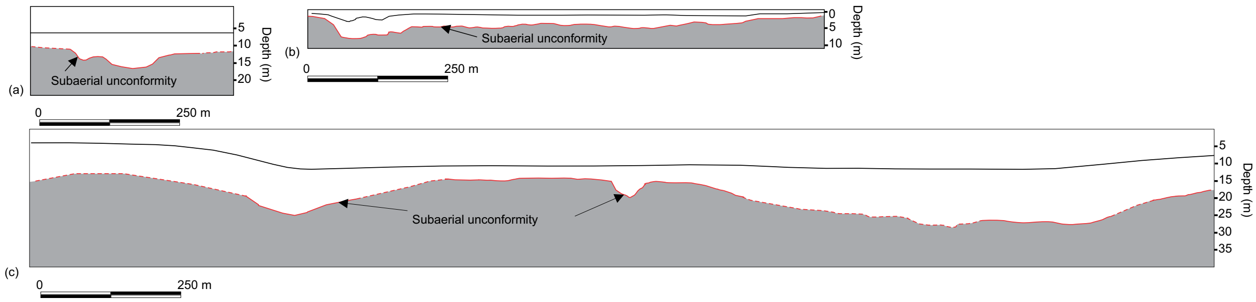
(a)
Subaerial unconformity
Depth (m)
5
10
15
20
0
250 m
(b)
Subaerial unconformity
Depth (m)
0
5
10
0
250 m
(c)
Subaerial unconformity
Depth (m)
5
10
15
20
25
30
35
0
250 m

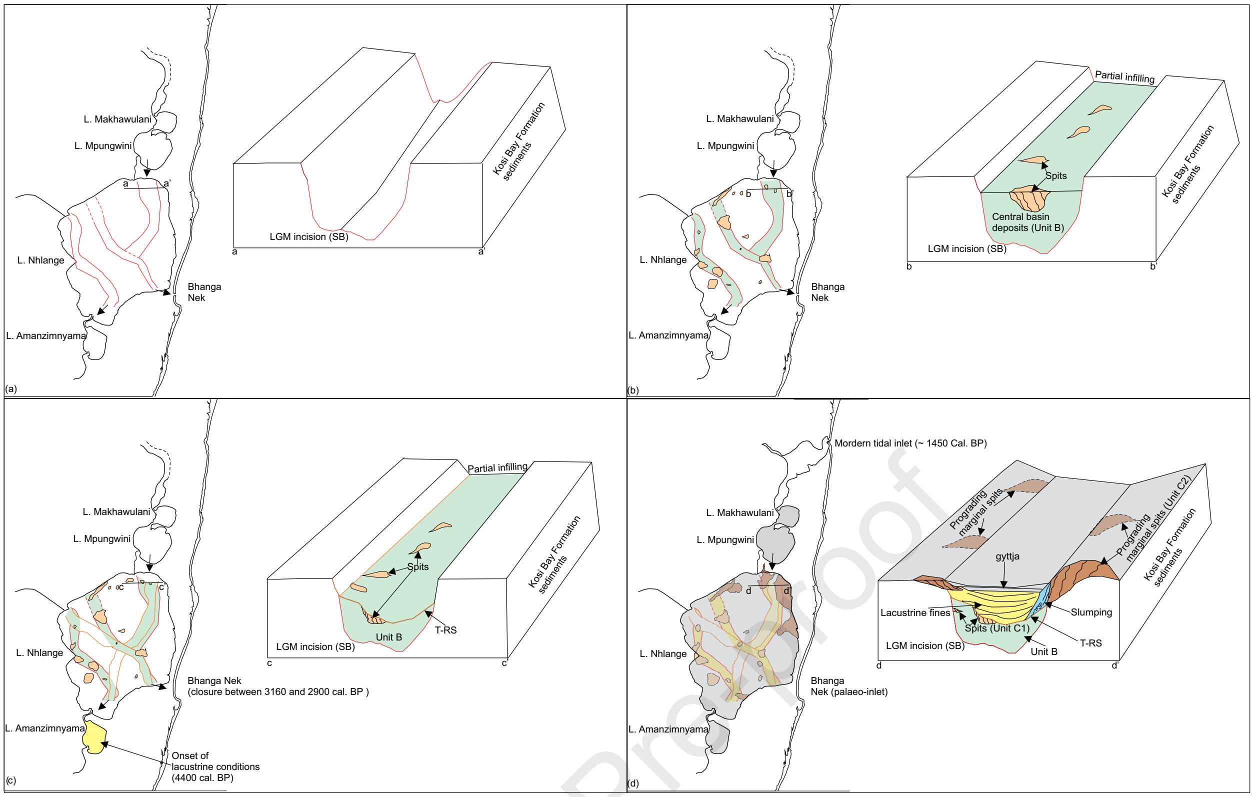

L. Makhawulani
L. Mpungwini
L. Nhlange
L. Amanzimnyama
Bhanga Nek
LGM incision (SB)
Kosi Bay Formation sediments
(a)
Partial infilling
Spits
Central basin deposits (Unit B)
(b)
Bhanga Nek (closure between 3160 and 2900 cal. BP )
Onset of lacustrine conditions (4400 cal. BP)
Unit B
T-RS
(c)
Mordern tidal inlet (~ 1450 Cal. BP)
Bhanga Nek (palaeo-inlet)
Prograding marginal spits
Prograding marginal spits (Unit C2)
gyttja
Lacustrine fines
Spits (Unit C1)
Slumping
(d)

- LGM-age incision into unconsolidated Kosi Bay Formation sediments
- Limited sediment supplied to the area during transgressing sea levels
- Post-LGM homogenous central basin fills only partially fill incised valleys
- Development of wind-driven spits signifying early stages of lagoonal segmentation
- Along-strike variation in the timing of the basin infilling

**Declaration of interests**

☒ The authors declare that they have no known competing financial interests or personal relationships that could have appeared to influence the work reported in this paper.

☐ The authors declare the following financial interests/personal relationships which may be considered as potential competing interests: